RSC Advances

ROYAL SOCIETY OF CHEMISTRY

www.rsc.org/advances

Journal Name RSCPublishing

ARTICLE

Supercritical fluid methods for synthesizing cathode materials towards lithium ion battery applications

Cite this: DOI: 10.1039/x0xx00000x

M.K. Devaraju*[a], Q.D. Truong[a], T. Tomai[a] and I. Honma*[a]

Received 00th January 2012,
Accepted 00th January 2012

DOI: 10.1039/x0xx00000x

www.rsc.org/

Lithium ion battery materials upraise the current technology to store electrical energy for the creation of green environment. The synthesis of lithium ion battery materials is crucial for the energy application in mobile electronic devices to plug-in hybrid electric vehicles. In this review, we summarize the recent progress made to synthesize lithium ion battery materials via supercritical fluid methods and particularly, its application towards the synthesis of layered transition metal oxides, spinel structured cathodes, lithium metal phosphates, lithium metal silicates and lithium metal fluorophosphates have been summarized. The cathode materials structure, particle size, morphology and electrochemical properties have been discussed. From the view of material synthesis, supercritical fluid methods are economical and have several advantages such as, phase purity, morphology control and size tuning down to 5 nm, which would greatly impact on the performance of lithium ion batteries.

1. Introduction

Lithium ion batteries are imperative energy storage technology for next generation of electronics, electrical and plug-in hybrid electric-electronic applications. Lithium ion batteries have highest energy density and highest operating voltage developed so far than any other current energy storage devices. There are innumerous advantages of lithium ion batteries such as great capacity retention, operation at wide range of temperatures, fair degree of safety on operations and so on.[1,2] Considering these benefits, the current technology can be upgraded to sustainable energy storage technology by improving the charge capacity, high rate performance, energy density and using environmentally benign process to produce lithium ion battery materials.[3] The property of battery materials depend on various factors such as well defined crystal structure, minimum defects, controlled composition, various particle size, and morphologies, which play key role in determination of the energy density, capacity retention, cyclic performance and safety of lithium ion batteries.[4,5]

Since, the discovery of layered transition metal oxides as cathode and graphite/hard as anode material, many new cathode and anode materials have been investigated. Till now, few cathode materials such as $LiCoO_2$ or $LiNi_{1-x-y}Co_xMn_yO_2$, $LiMn_2O_4$ and $LiFePO_4$ were intensively studied.[6] $LiCoO_2$ or $LiNi_{1-x-y}CoxMnyO_2$ cathode materials have several advantages such as high specific capacity, high operating voltage, long cycle life and easy to synthesize.[6a,6b] The oxygen evolution at high operating voltage make them serious for high voltage applications. $LiMn_2O_4$ is also exhibit several advantages, such as low cost, high rate performance and higher abundance of Mn and good thermal stability, therefore it is considered as good cathode candidate for power tool applications.[6c, 6d] After the investigation of $LiFePO_4$ by J. B. Goodenough,[6e] $LiFePO_4$ olivine structured cathode material has been widely studied due to its excellent characteristics such as cycle stability, low cost, environmentally benign and easy to manufacture which make this material as a most potential cathode for lithium ion batteries. However, the properties of cathode materials depend on synthesis methodology, nature of starting materials, reaction media, and reaction kinetics. Moreover, phase purity, homogeneity, particle size, morphology and cation order amongst other critical parameters infer the performance of batteries.[3] Recently, orthosilicates and fluorophosphates, are being explored for energy storage applications.[7,8]

In recent years, several synthetic routes have been developed to produce variety of cathode and anode materials. From longtime, solid state reaction has been widely used to synthesize lithium ion battery materials.[6e,9] Solid state reaction involves mixing of metal oxides or carbonates and heat treatment at high temperature for long time, which consumes lot of energy, time and moreover, obtained products show inhomogenity, impurity, and larger particle size. The challenges in terms of materials design for lithium ion battery will continue, the development of novel and advanced energy storage materials with various size, shape and three dimensional nano/microstructures with excellent performance are most important challenges in materials design for lithium ion battery. The new materials

design is the main focus of many prominent research group in the field of electrode materials design across the world.

Recently , various methods have been developed to prepare lithium battery materials such as the sol–gel method,[10,11] co-precipitation,[12,13] mechanochemical activation,[14,15] spray technology.[16]

However, all these methods have limitations when it comes to a practical point of view. Therefore, solution processes such as hydrothermal, solvothermal, ion exchange and supercritical fluid methods have been intensively studied.[17] Amongst solution processes for the synthesis of electrode materials, supercritical fluid methods attracts due to its novel opportunities to design inorganic functional materials with variety of shapes, size, hierarchical structures and which ensures the one pot synthesis.[18] Supercritical fluid methods is commercially viable process, which reduces the energy consumptions and certainly applicable to large scale synthesis.

In this review, we summarize the progress of supercritical fluid methods towards the development of lithium ion battery materials, such as lithium transition metal oxides, lithium metal phosphates, fluorophosphates and lithium metal silicates.

2. Supercritical fluid methods

Supercritical fluid can be any substance at critical point of given temperature and pressure of that substance (**Fig 1A**). If water is a substance, the critical point of water is 374 ^{o}C, above this temperature water turns out to be supercritical fluid. Supercritical fluids exhibit number of advantages, which allow us to fine tune the reaction kinetics or reaction atmosphere by just varying the pressure and temperatures. The physicochemical properties such as density, viscosity, diffusivity or surface tension can be easily modified as we required. Supercritical fluid can effectively diffuse through the solids like a gas and dissolve the solids like a liquid. These properties can be exploited for materials synthesis with various kinds of shape and size.[18,19]

Compared to various synthetic methodology from high temperature solid state reaction method to low temperature hydrothermal/solvothermal process, supercritical fluid methods have been considered as green and environmentally benign process because of numerous merits (**Fig. 1B**). First, the time requirement for materials synthesis is from few minutes (continuous synthesis) to less than few hours (batch synthesis), it reduces the energy consumption and time. The synthesis temperature will be less than 500 ^{o}C depending upon the type of materials processing, which reduces the energy consumption and price. The particles with less than few nanometer size can be synthesized, where size can define the property of materials. This process is relatively low temperature process and easily applicable to large scale synthesis. Recently large scale synthesis of $LiFePO_4$ electrode materials with 1000 tones/year is initiated by Hanwa chemical, Korea.

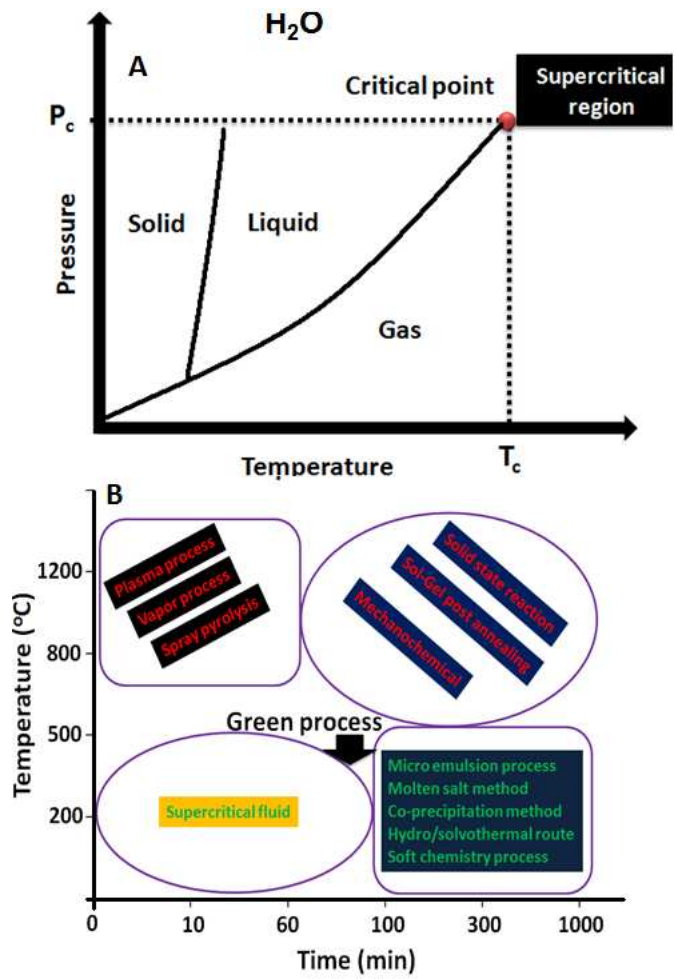

Fig. 1 (A) Substance (water) at supercritical region with changing temperature and pressure, (B) comparison of supercritical fluid method with other synthetic methodology.

Supercritical fluid methods for synthesizing cathode materials and their properties are listed in **Table 1**.

3. Lithium transition metal oxides

Lithium transition metal oxides are considered as most efficient cathode and anode materials for lithium ion batteries. There are various transition metals oxides such as, $LiCoO_2$, $LiNiO_2$, $LiMn_2O_4$, $LiNi_{1-x-y}Co_xMnyO_2$ $Li_{4/3}Ti_{5/3}O_4$, and so on. Few metal oxides such as $LiCoO_2$ and $LiMn_2O_4$ have been successfully commercialized for lithium ion battery applications.

The supercritical fluid methods for synthesis of lithium transition metal oxides was realized by K. Kanamura et al[20] in 2000 and T. Adschiri et al[21] in 2001. K. Kanamura et al have used flow type supercritical water synthesis for the synthesis of $LiCoO_2$ particles. For the flow type synthesis of $LiCoO_2$ particles, aqueous solutions of LiOH, $Co(NO_3)_2$ and distilled water or H_2O_2 were fed into the preheated supercritical chamber in three different line as shown in **Fig. 2A**. The synthesis was completed in 1 min and the XRD of as-synthesized particles showed layered rock type crystal structure as shown in **Fig. 2B**. The XRD of $LiCoO_2$ was compared with

that of the $LiCoO_2$ prepared via solid state reaction method. The slight difference in diffraction intensities were noticed. However, pure phase of $LiCoO_2$ was successfully synthesized via flow type supercritical water method. Scanning electron microscopy images of $LiCoO_2$ synthesized via flow type supercritical water is shown in **Fig. 2C**. The $LiCoO_2$ particles with size of 1μm in diameter was successfully synthesized. They also mention that, the particles size can be controlled to few nanometer by changing the reaction conditions.

Adschiri et al[21] have used both batch type and flow type supercritical method to synthesize $LiCoO_2$ particles. The starting materials such as LiOH and $Co(NO_3)_2.6H_2O$ were used.

For the batch type synthesis, the mixture of aqueous solutions of LiOH and $Co(NO_3)_2$ were loaded into the batch type reactor as shown in **Fig. 3**.

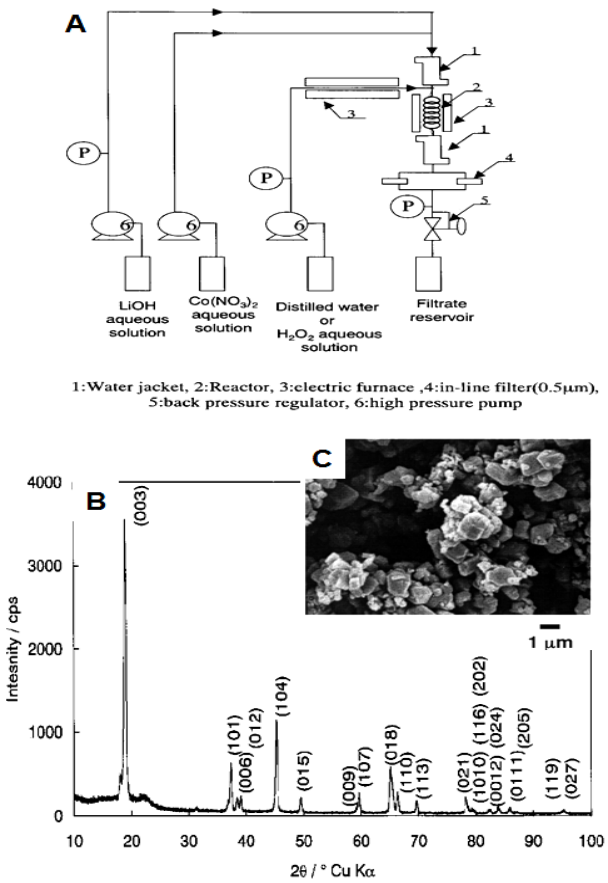

Fig. 2 (A) Flow type supercritical water synthesis, (B) XRD pattern of $LiCoO_2$ particles, and (C) SEM image of $LiCoO_2$ particles.(Reprinted with permission from Electrochemical and Solid-State Letters.)[20]

The synthesis was carried out at 400 °C and the pressure at 30 MPa in presence of oxygen gas. They showed that single phase of $LiCoO_2$ can only be obtained at supercritical condition in presence of oxygen gas, to oxidize all the divalent cobalt ions into trivalent cobalt in synthesized $LiCoO_2$. The $LiCoO_2$ particles synthesized via flow type supercritical method show smaller particles with particles diameter ranging from 600 nm to 1μm, whereas the particles synthesized via batch type supercritical method show larger particles with 2-3 μm in size with clear single crystal appearance.

The electrochemical analysis for $LiCoO_2$ particles synthesized via flow type supercritical hydrothermal method was carried out. For the electrochemical analysis, mixed solvent of ethylene carbonate and diethylene carbonate containing 1M of

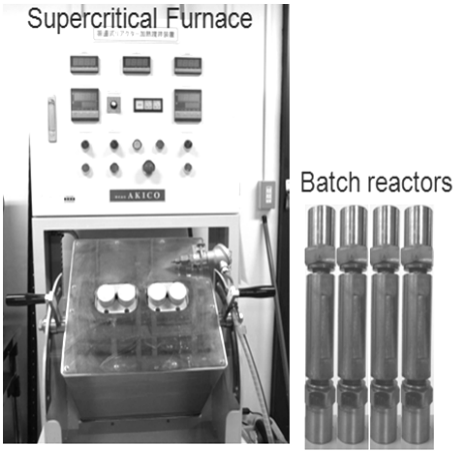

Fig. 3 Batch type supercritical method used in Honma lab, at Tohoku university.

$LiClO_4$ was used as electrolyte. The stable discharge capacities of 110 mA h g^{-1} is obtained at 0.1mA current density and authors claimed that the stable cyclic performance is due to the single crystalline $LiCoO_2$ particles.

Y.H. Shin et al[22] have used continuous hydrothermal method to synthesize $LiCoO_2$ particles under supercritical water conditions. The effect of temperature, residence time, lithium hydroxides and hydrogen peroxide has been investigated. LiOH and $Co(NO_3)_2.6H_2O$ were used as starting materials. **Fig. 4A** shows the XRD pattern of as-synthesized $LiCoO_2$ particles at various residence time of less than 1 min at 400-404°C and 300 bar pressure, with different concentration of LiOH and $Co(NO_3)_2$. The XRD pattern shows well developed HT-$LiCoO_2$ phase without any undesired product, the intensity of diffraction peaks increased with the time. The results confirmed that pure phase of $LiCoO_2$ can be synthesized at continuous hydrothermal conditions. The author noticed that, use of excessive amount of LiOH and H_2O_2 was beneficial to synthesized single phase $LiCoO_2$ particles under supercritical conditions. The authors claim that, the residence time of this particle preparation is less than any other synthesis reports. The as-synthesized particles showed particles size between 300-500 nm with similar morphologies as shown in **Fig. 4B-4E**. Please refer this article for detail information on investigation of $LiCoO_2$ particles by changing various parameters. The authors have not measured the charge-discharge measurements for synthesized particles. This report shows that $LiCoO_2$ size can be controlled by controlling various parameters.

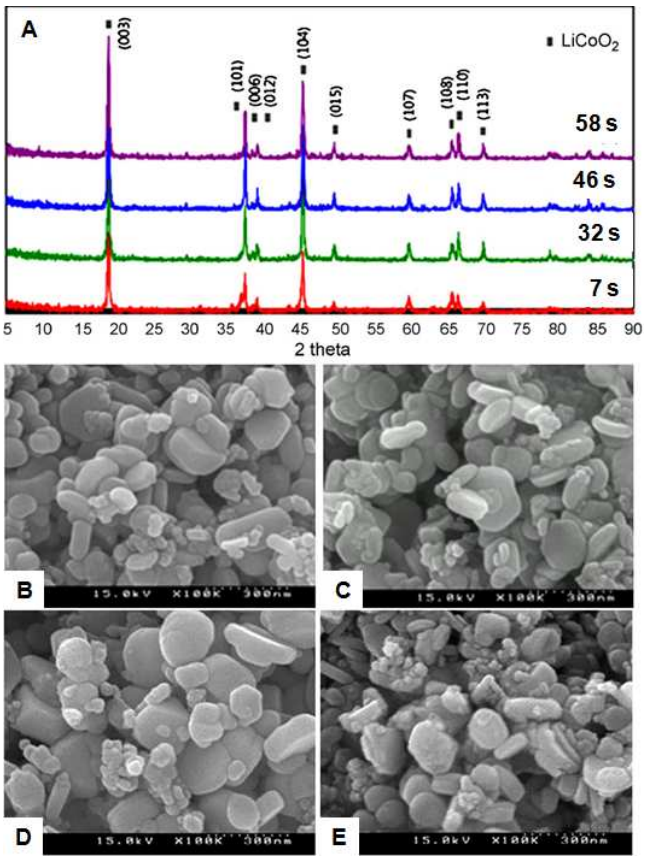

Fig. 4 (A) XRD patterns of $LiCoO_2$ synthesized at 400-404 ^oC at different residence time, (B)-(E) SEM images of $LiCoO_2$ particles synthesized by batch type supercritical method.(B) and (C) using 0.4M LiOH, 0.02M $Co(NO_3)_2$, 0.02MH_2O_2 time: 46s and 58s respectively. (D) at 400 ^oC and (E) 411 ^oC. (Reprinted with permission from Elsevier Ltd.)[22]

In 2005, K. Kanamura et al[23] have used hydrothermal process in supercritical water with heat treatment to synthesize $LiMn_2O_4$ cathode materials for rechargeable lithium batteries. The synthesis was carried out in stainless steel cylindrical–type vessel (inner volume 10 mL). For the synthesis, aqueous solutions of LiOH and $Mn(NO_3)_2$ were used with water in 3:1 molar ratio. The reaction was carried out with or without H_2O_2 at 400 ^oC for 15 min and at inside pressure of 30 MPa. $LiMn_2O_4$ was also synthesized by solid-state reaction method for the comparison. **Fig. 5A** shows the XRD pattern of as-synthesized $LiMn_2O_4$ cathode material with various ratios of LiOH: $Mn(NO_3)_2$: H_2O_2. In all the cases, the obtained sample was $LiMn_2O_4$ and the diffraction peaks are well compared to that of spinel $LiMn_2O_4$. The peak of Mn_3O_4 as impurity was observed for the sample synthesized without H_2O_2. However, no impurity was found for the samples prepared in presence of H_2O_2. The authors claimed that, adding H_2O_2 into supercritical water was effective to synthesize single phase spinel $LiMn_2O_4$. The SEM images displayed in **Fig. 5B** are $LiMn_2O_4$ prepared with various H_2O_2 ratios. They found that, not much difference in the particle size and shapes for the samples prepared with or without H_2O_2. When high concentration of H_2O_2 was used in the synthesis, the synthesized samples had smaller size due to the influence of H_2O_2 on the nucleation process of $LiMn_2O_4$. The particles showed few hundred nanometers in size with similar shape.

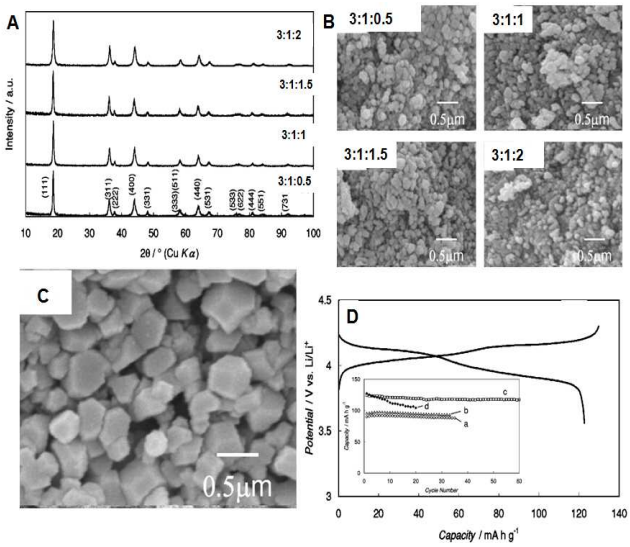

Fig. 5 (A) XRD pattern and (B) SEM images of $LiMn_2O_4$ synthesized at 400^oC at different ratio of LiOH:$Mn(NO_3)_2$:H_2O_2, (C) $LiMn_2O_4$ particles after heat treated at 800 ^oC for 1h, (D) Charge-discharge profile of $LiMn_2O_4$ particles after heat treated at 800^oC for 1h (inset Figure: cyclic performances of heat treated samples (a) 400^oC, (b) 600 ^oC (c) 800^oC and (d) $LiMn_2O_4$ synthesized by solid-state reaction. (Reprinted with permission from Journal of the Electrochemical Society.)[23]

The authors have not observed good charge-discharge performance for $LiMn_2O_4$ cathode materials shown in **Fig. 5A** and **Fig. 5B**. So that, heat treatment was carried out in order to improve the electrochemical performance, authors heat treated the sample at various temperatures (400-800^oC). **Fig. 5C** shows the SEM images of $LiMn_2O_4$ particles heat treated at 800^oC for 1 h, which shows well defined crystals with 500 nm in size and almost the particles look like single crystals. The authors noticed that, particles size and shape changed with the heating temperatures. The charge-discharge profile of $LiMn_2O_4$ particles heat treated at 800 ^oC for 1 h shown in **Fig. 5D** with good cyclic performance (inset figure in **Fig. 5D**). For the electrochemical measurement, 1M $LiClO_4$/EC+DEC was used as electrolyte. The discharge capacity of more than 125 mA h g^{-1} at 0.1C with good cyclic performance. The observed capacity was comparable with that of sample synthesized via solid state reaction. The authors claimed that, the discharge capacity is improved due to the high crystallinity and crystallite size because of heat treatment which leads to improved electrochemical performances.

In 2006, Joo-Heon Lee et[24] al have attempted to synthesize $LiMn_2O_4$ particles in supercritical water using flow type synthesis method with residence time of 30-40s. The authors have investigated, the selective synthesis of $LiMn_2O_4$ is mainly

dependent on the amount of OH^- ion in the reactants. The author synthesized $LiMn_2O_4$ particles using $Mn(NO_3)_2.6H_2O$, LiOH, KOH, $LiNO_3$ solutions at 420 °C and 300 pressure bar.

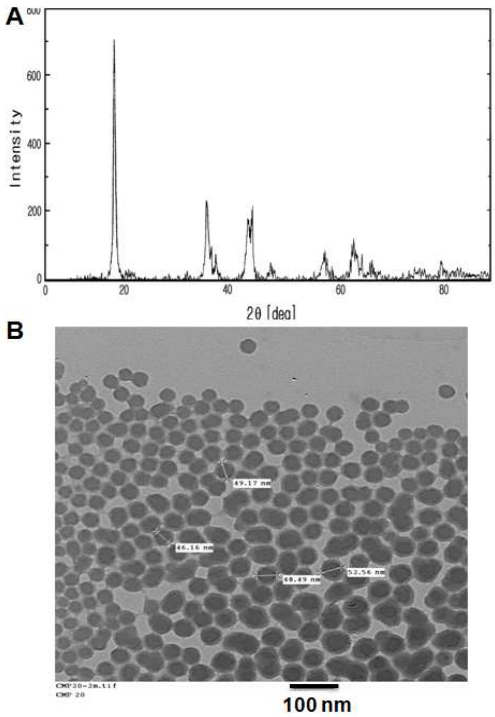

Fig. 6 (A) XRD pattern and (B) TEM image of $LiMn_2O_4$ synthesized using 0.1mol/L of LiOH and Li/Mn=4. (Reprinted with permission from Korean J. Chem. Eng.)[24]

Fig. 6A shows the XRD pattern of $LiMn_2O_4$ particles synthesized using 0.1mol/L of LiOH and Li/Mn=4. They observed that, single phase of $LiMn_2O_4$ particles can be synthesized using high concentration of LiOH (0.1mol/L) and not with $LiNO_3$ or LiOH/$LiNO_3$ mixtures. The TEM image of $LiMn_2O_4$ synthesized using 0.1mol/L of LiOH and Li/Mn=4.shown in **Fig. 6B**. The particles showed sphere shape with particles size less than 100 nm. The authors have not characterized electrochemical performances of $LiMn_2O_4$ particles.

Recently, Jae-Wook Lee et al[25] have synthesized $LiCoO_2$, overlithiated $Li_{1.15}CoO_2$ and $LiNi_{1/3}Co_{1/3}Mn_{1/3}O_2$ cathode materials using batch type supercritical water method in presence of argon or oxygen gas. LiOH and $Co(NO_3)_2.6H_2O$ were used as starting materials to synthesize $LiCoO_2$ and $Li_{1.15}CoO_2$. For the synthesis of $LiNi_{1/3}Co_{1/3}Mn_{1/3}O_2$, LiOH, $Ni(NO_3)_2.6H_2O$, $Co(NO_3)_2.6H_2O$ and $Mn(NO_3)_2.6H_2O$ were used as starting materials and KOH solution was used to vary the PH of the solution. The synthesis was carried out at 400 °C for 10 min of reaction time.

Fig. 7A shows the XRD pattern of as-synthesized $Li_{1.15}CoO_2$ and $LiNi_{1/3}Co_{1/3}Mn_{1/3}O_2$ cathode materials using KOH solution and purge oxygen gas at 400 °C for 10 min of reaction time.

The observed diffraction peaks were indexed as a layered oxide structure based on a hexagonal α-$NaFeO_2$ structure (space group: *R-3m*). The XRD patterns of $LiNi_{1/3}Co_{1/3}Mn_{1/3}O_2$ is similar to that of $Li_{1.15}CoO_2$ and they exhibited a layered structure.

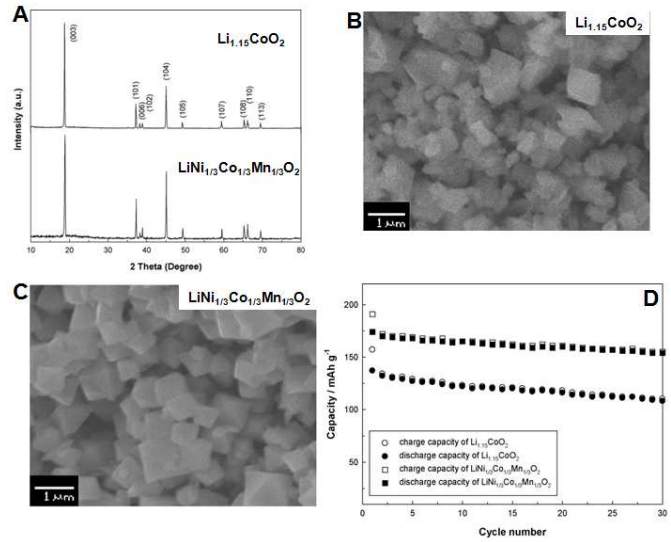

Fig. 7 (A) XRD patterns, (B) & (C) SEM images of $Li_{1.15}CoO_2$ and $LiNi_{1/3}Co_{1/3}Mn_{1/3}O_2$ particles synthesized by supercritical water with KOH solution and purge oxygen gas at 400°C for 10 min. (D) Cyclic performance of $Li_{1.15}CoO_2$ and $LiNi_{1/3}Co_{1/3}Mn_{1/3}O_2$ particles. (Reprinted with permission from Elsevier Ltd.)[25]

Fig.7B and & **7C** shows the SEM images of $Li_{1.15}CoO_2$ and $LiNi_{1/3}Co_{1/3}Mn_{1/3}O_2$ cathode materials prepared with an aqueous KOH solution and oxygen purge gas. The particles showed 300 nm to 1μm in size with cubic shape and they exhibited clear crystal boundaries without hard agglomerations. The authors observed initial discharge capacities of 149 and 180 mA h g^{-1} for $Li_{1.15}CoO_2$ and $LiNi_{1/3}Co_{1/3}Mn_{1/3}O_2$ particles at current density of 16 mA g^{-1} at room temperature. The cyclic performance was measured within voltage window of 2.5-4.5V for $Li_{1.15}CoO_2$ and $LiNi_{1/3}Co_{1/3}Mn_{1/3}O_2$ at 80 mA h g^{-1} for 30 cycles are shown in **Fig.7D,** where $LiNi_{1/3}Co_{1/3}Mn_{1/3}O_2$ cathode materials so better cyclability than $Li_{1.15}CoO_2$ particles the author claims that better cyclability of $LiNi_{1/3}Co_{1/3}Mn_{1/3}O_2$ cathode material is due to the characteristics of cathode powders. The authors have also investigated the rate performance of both $Li_{1.15}CoO_2$ and $LiNi_{1/3}Co_{1/3}Mn_{1/3}O_2$ particles.1M$LiPF_6$ in a mixture of ethylene carbonate (EC) and diethyl carbonate (DEC) in a 1:1 volume ratio was used as electrolyte. The above discussed research work shown the importance of supercritical fluid techniques in preparation of layered oxide materials with controlled composition, size, morphology and also to improve the electrochemical properties. Further research has to be carried out on layered metal oxides and spinel structure materials. The coating of metal or doping

Table 1. Cathode materials synthesized by supercritical

of effective cations could improve the capacity of these materials with enhanced cyclability. The observation of full theoretical capacity of these materials could be possible via different approaches by controlling structure, size and morphology.

4. Lithium metal phosphates

After the pioneer work of Goodenough et al[6e] on $LiFePO_4$ olivine structured cathode material, lithium metal phosphates $LiMPO_4$, M=Fe, Mn, Co and Ni) have received great attention as an excellent candidate for lithium ion battery applications. In the last two decades, $LiMPO_4$ cathode materials have been extensively investigated, particularly $LiFePO_4$ material are tremendously investigated as potential cathode to replace $LiCoO_2$ because of its low cost, non toxic and high theoretical capacity. $LiFePO_4$ has been already commercialized for energy storage applications. Olivine structured $LiMPO_4$ are still being investigated by many researchers.

	Materials	System	P/T MPa/°C	Particle size (nm)	Morphology	Capacity ($mAhg^{-1}$)	Ref
Transition metal oxides	oxides						
	$LiCoO_2$	Continuous	30/400	900-1000	Rough shape	N.A.	(20)
	$LiCoO_2$	Batch	30/400	2000-3000	Rough shape	N.A	(21)
	$LiCoO_2$	Continuous	N.A./300-400	600-1000	Rough shape	N.A.	(21)
	$LiCoO_2$	Continuous	30/400	100-300	Nanoplates	N.A.	(22)
	$LiMn_2O_4$	Batch	30/400	300-500	Spherical	130	(23)
	$LiMn_2O_4$	Continuous	30/380	50-300	Irregular shape	N.A.	(24)
	$LiNCMO_2$	Batch	30/400	600-1000	Pyramid	180	(25)
Phosphates							
	$LiFePO_4$	Batch	33.5/300-400	500-1200	Irregular shape	N.A.	(26a)
	$LiFePO_4$	Batch	30/389	100	Spherical/rod	140	(26b)
	$LiFePO_4$	Continuous	N.A./300-385	50-130	Spherical	N.A.	(26c)
	$LiFePO_4$	Continuous	25/400	20	Spherical	75	(27)
	$LiFePO_4$	Batch	40/400	15	Spherical	165	(28)
	$LiFePO_4$	Batch	40/400	50x200	Rod-Hierarchy	152	(29)
	$LiFe/MnPO_4$	Batch	40/400	20x100	Nanorods	158	(30,31)
	$LiMnPO_4$	Batch	40/400	20x100	Nanorods	158	(30,31)
	$LiFePO_4$	Continuous	25/400	25	irregular	105	(32,33)
	$LiFePO_4$	Batch	N.A./400	50x2000	Spindle	138	(34)
	$LiFePO_4$	Batch	25/100	2000	Porous	162	(35)
	$LiFePO_4$	Batch	10/400	3.7-4.6(b-axis)	Nanosheets	164	(37)
	$LiMnPO_4$	Batch	10/400	3.7-4.6(b-axis)	Nanosheets	157	(37)
	$LiCoPO_4$	Batch	10/400	3.7-4.6(b-axis)	Nanosheets	153	(37)
	$LiCoPO_4$	Batch	40/400	5-15(b-axis)	Nanoplates	135	(38a)
	$LiCoPO_4$	Batch	40/400	50x1000	Nanorods	130	(38b)
	$LiCoPO_4$	Batch	40/400	50x200	Nanoplates	121	(38b)
Silicates							
	Li_2FeSiO_4	Batch	40/400	1-5	Nanosheets	340	(42)
	Li_2MnSiO_4	Batch	40/400	1-5	Nanosheets	350	(42)
	Li_2MnSiO_4	Batch	N.A./300	10	Spherical	313	(43)
	Li_2MnSiO_4	Batch	38/400	500	Hierarchy	292	(44)
	Li_2FeSiO_4	Batch	38/400	50x400	Nanorods	177	(45)
	Li_2CoSiO_4	Batch	38/350	200	Irregular shape	107	(46)

NA: Not Available

In 2005, J. Lee et al[26a] have reported supercritical water synthesis of $LiFePO_4$ particle using batch type reactors. $LiFePO_4$ was synthesized from $FeSO_4$ $7H_2O$, H_3PO_4 and LiOH by dissolving in distilled water. The synthesis was carried out in a 250 ml stainless steel autoclave. The authors have investigated, effect of temperature, time, pH and reactants concentrations on morphology and size of $LiFePO_4$ particles. **Fig. 8A** shows the XRD patterns of $LiFePO_4$ synthesized at various temperatures. All the diffraction peaks are comparable with the standard pattern (JCPDS 40-1499). The XRD pattern was compared with some of published reports. They observed increased peak intensity with increasing the reaction temperatures. They observed changes in morphology of $LiFePO_4$ particles. **Fig. 8B** shows the SEM image of $LiFePO_4$ particles synthesized at 387 °C for about 1h. The obtained particles are smaller and softly agglomerated with uniform shape, when compared to the particles synthesized at low and subcritical temperatures.

Again in 2006, the same group[26b] have reported $LiFePO_4$ micro and nanoparticles in supercritical water. Two kind of synthesis routes were employed to synthesized micro and nanoparticles. In synthesis A, authors used acidic stock

solutions of Li_3PO_4 and *o*-H_3PO_4 and basic stock solution of NH_4OH in distilled and deionized water to obtain any desired pH. The stock solutions and 3.75 g of $FeSO_4.7H_2O$ granules were added to the autoclave and argon gas. Following reaction was expected:

$Li_3PO_4 + 2H_3PO_4 + 3(FeSO_4.7H_2O) + 6NH_4OH \rightarrow 3LiFePO_4 + 3(NH_4)_2SO_4 + 27H_2O$.

After 1 h, the reaction was finished. SEM images of obtained particles at are shown in Fig. 8C. These particles were obtained at 389 °C with pH 5.26. The micron sized particles with rod like morphology was observed.

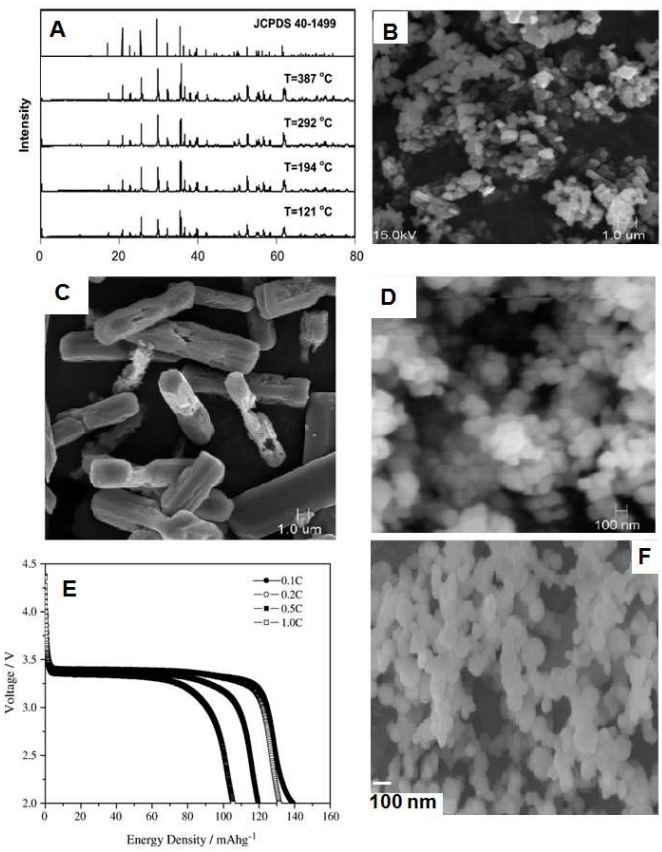

Fig. 8 (A) XRD patterns of $LiFePO_4$ synthesized at different temperatures, (B) SEM image of $LiFePO_4$ synthesized at 387 °C for 10 min, (Reprinted with permission from Elsevier Ltd.) [26a] (C) & (D) SEM images of $LiFePO_4$ synthesized at 389 °C via reaction A and reaction B respectively, (E) discharge profile of $LiFePO_4$ shown in Fig.8D (Reprinted with permission from Elsevier Ltd.)[26b] and (F) $LiFePO_4$ particles synthesized via continuous hydrothermal synthesis. (Reprinted with permission from Elsevier Ltd.) [26c]

In synthesis route B, the authors used NaOH solutions to control pH and Li_3PO_4 was employed as a source for both lithium and phosphate ions. For synthesize, 150 ml of an aqueous solution of $FeSO_4 \cdot 7H_2O$ was prepared and NaOH solution was added to adjust the pH of the resulting mixture to any desired value. Then the experiments were carried out. The synthesis reaction was summarized as follows;

$Li_3PO_4 + FeSO_4.7H_2O \rightarrow LiFePO_4 + 3(NH_4)_2SO_4 + LiSO_4 + 7H_2O$.

Fig. 8D shows the SEM images of $LiFePO_4$ particles with particle size less than 100 nm. The author observed that, temperature was the dominant factor and pH apparently had little effect on particle size and shape. The author investigated electrochemical analysis for $LiFePO_4$ particle obtained via synthesis route B. The discharge capacities measure at various current densities are shown in Fig. 8E. The discharge capacity of 140 mA h g^{-1} at 0.1C was observed and 75% of this capacity was maintained at 1C, which is correspond to 82% of the theoretical capacity. The author claims that, the observed capacity is higher than $LiFePO_4$ synthesized from other methods.

C. Xu et al[26c] have proposed a continuous hydrothermal synthesis of $LiFePO_4$ particles in subcritical and supercritical water. They used flow type reactors, where degassed solutions of $FeSO_4$ in H_3PO_4 (solution 1) and LiOH (solution 2) were contacted with hot, compressed water (solution 3) in a mixing tee, resulting in the precipitation of $LiFePO_4$ particles according to the reaction:

$FeSO_4 + H_3PO_4 + 3LiOH \rightarrow LiFePO_4 + Li_2SO_4 + 3H_2O$

The authors have investigated the effect of temperature, water flow rate, concentration and also compared batch type synthesis with flow type hydrothermal synthesis. **Fig. 8F** shows an SEM image of $LiFePO_4$ particles about 40 nm in size which are obtained by continuous hydrothermal synthesis. This method has advantages on controlling the crystal size below 50 nm, however, the author have not shown electrochemical performance of this material.

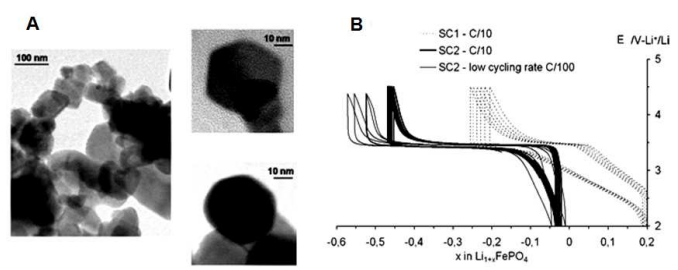

Fig. 9 (A) TEM images of particles obtained by continuous hydrothermal synthesis, b) galvanostatic cycling of hydrothermally synthesized $LiFePO_4$ at two reaction times: SC1 6 s and SC2 12 s, with charge–discharge rates of C/10, SC2 with a low cycling rate of C/100. (Reprinted with permission from Elsevier Ltd.)[27]

In 2009, A. Aimable et al[27] have used similar method to synthesize $LiFePO_4$ nanoparticles. For the synthesis, reactive solution 1 was prepared by dissolving $(NH_4)_2Fe(SO_4)_2.6H_2O$ (19.6 g, 0.1 mol L^{-1}) and o-H_3PO_4 (4.9 g, 0.1 molL^{-1}) in deionized water (500 mL). Reactive solution 2 was prepared by dissolving LiOH, H_2O (7.8 g, 0.375 mol L^{-1}) in deionized water

(500 mL).TEM images of particles obtained by continuous hydrothermal synthesis shown in **Fig. 9A**, the particles show 50 nm in diameter with clear crystal habit. The electrochemical property was measured for two samples namely SC1 composed of aggregated particles (reaction time 6 s) and SC2 composed of non agglomerated particles (reaction time 12 s). The electrode made from sample SC2 exhibited a unique flat charge and discharge curve at 3.5 V, with almost no polarization (**Fig. 9B**). It was observed that, 0.45 Li were inserted reversibly in this material, corresponding to a capacity of 75 mA h g^{-1}. The authors have demonstrated that 50 nm size particles can be synthesized with good electrochemical performance.

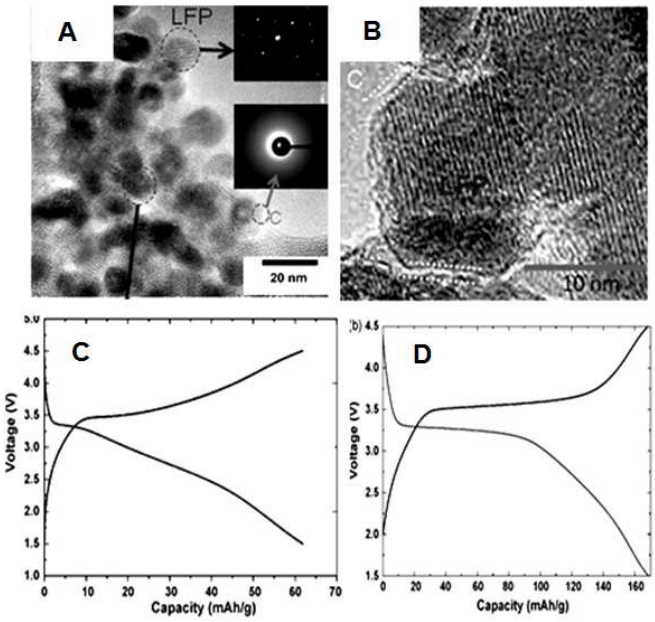

Fig. 10 (A) TEM images of $LiFePO_4$ particles obtained by in the presence of organic molecules. Inset: electron diffraction pattern of nanocrystals and amorphous carbon (B) HR-TEM image showing lattice fringes, (C) Charge-discharge profile of as-synthesized $LiFePO_4$ and (D) heated $LiFePO_4$ (Reprinted with permission from Elsevier Ltd.)[28]

In 2009, surface modified $LiFePO_4$/C nanocrystals using supercritical batch reactors has been reported by our group[28]. *In-situ* carbon coated $LiFePO_4$/C nanocrystals were synthesized using $FeC_2O_4 \cdot 2H_2O$, $NH_4H_2PO_4$, LiOH, ascorbic acid and oleic acid as starting materials. Ethanol was used as solvent. The synthesis was carried out at400 °C for about 10-30min. The HR-TEM images of as-synthesized $LiFePO_4$ nanocrystals in the presence of organic molecules under supercritical water conditions are shown in **Fig. 10.** $LiFePO_4$ nanocrystals show 15 nm in diameter which is synthesized in presence of oleic acid, which play a key role in controlling the particle size (**Fig. 10B**). The distinct lattice planes are shown in Fig. 10B and the SAED

In 2010, directed growth of nanoarchitectured $LiFePO_4$ electrode by solvothermal synthesis using batch reactors at supercritical fluid condition was reported by our group[29]. In the synthesis, ethylene glycol as solvent and oleic acid or hexane was used as co-solvent. The synthesis was carried out at 400 °C for 10 min.

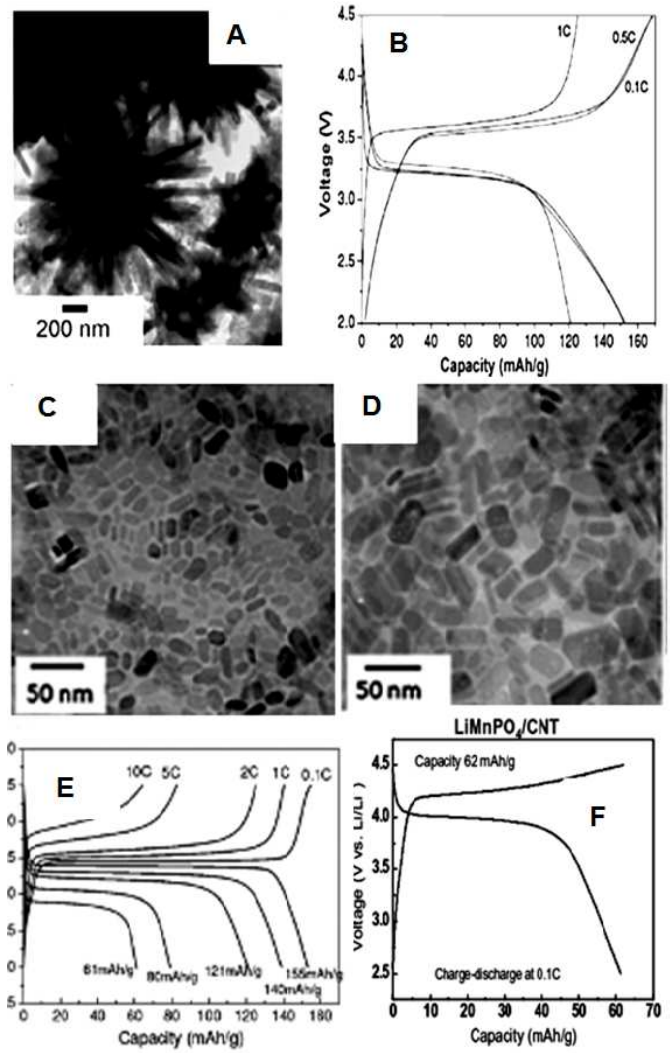

Fig.11(A) TEM image of a $LiFePO_4$ nanostructure synthesized in EG–oleic acid and (B) charge–discharge profile of $LiFePO_4$ at different current densities. (Reprinted with permission from Elsevier Ltd.)[29] (C) TEM images of $LiFePO_4$, (D) $LiMnPO_4$ particles synthesized in the presence of oleylamine, (E) charge–discharge profiles of $LiFePO_4$ at different current densities, and (F)Charge–discharge profile of $LiMnPO_4$ particles. (Reprinted with permission from The Royal Society of Chemistry.)[30]

Fig. 11A shows the TEM images of nano flower like structures with length ranging from 200-400 nm and width less than 100 nm in diameter. Different kinds of morphologies were obtained by changing the organic solvents. **Fig. 11B** shows the charge discharge profile of $LiFePO_4$ after heated at 600 °C. The flower like microstructure exhibits capacity as high as 154 mA h g^{-1}, with slope like plateau showing the effect of nanosize particles due to high surface area. The ED pattern shown in **Fig. 10A** (top inset) with bright spots of well defined diffraction pattern of olivine phase suggests that the well crystalline $LiFePO_4$/C

nanocrystals. The SAED showed in **Fig. 10A** reveal that $LiFePO_4$ nanocrystals are single crystalline. **Fig. 10C** shows the charge discharge profile of as-synthesized $LiFePO_4$ nanocrystals, which show small capacity, and then $LiFePO_4$/C nanocrystals were heated at 500 °C to have conductive carbon coating, after heat treatment $LiFePO_4$/C nanocrsytals showed improved discharge capacity (**Fig. 10D**). This process demonstrated on controlling the crystal size less than 20 nm with uniform shape and to have better electrochemical performance upon heating.

Followed by this work, in 2010, supercritical ethanol process to prepare $LiMPO_4$ (M= Fe and Mn) colloidal nanocrystals has been proposed by our group[30]. In a typical synthesis metal chloride dissolved in oleylamine and ethanol at 60 °C for 1 h followed by addition of *o*-H_3PO_4 solution and Li acetyl acetonate. The supercritical reaction was carried out at 250-400 °C for 4-10 min. **Fig. 11C** and **11D** shows the colloidal nanocrytals of $LiFePO_4$ and $LiMnPO_4$ with nanoplates and nanorods like morphology, respectively. The colloidal particles showed 15-20 nm in diameter in presence of oleylamine and in absence of oleylamine particles showed 70-90 nm in diameter. The use of oleylamine played an important role in reducing the particle size as it can absorb the specific crystal planes and inhibit the crystal growth under supercritical conditions. **Fig. 11E** and **11F** shows the charge discharge profile of $LiMPO_4$ (M= Fe and Mn) colloidal nanocrystals after conductive polymer coating and heat treatment. $LiFePO_4$ nanocrystal exhibited highest capacity of 158 mA h g^{-1} at 0.1 C rate, whereas $LiMnPO_4$ nanocrystals exhibited 62 mA hg^{-1} at 0.1 C. Further, to improve the discharge capacities of $LiMnPO_4$ nanocrstyal, a detail investigation was reported in 2011 from our group.[31] Where, the discharge capacities changes with the size of the particles. The discharge capacity of 123 and 92 mA h g^{-1} is obtained for 100 and 80 nm particle size, where as high discharge capacity of 152 mA h g^{-1} is obtained for 20 nm size $LiMnPO_4$ nanocrystals. The results shows that, proper conductive carbon coating of colloidal nanocrystals could exhibit full discharge capacity. The supercritical method using batch reactors in presence of selected starting materials and solvents has the potential to synthesize nanosize lithium battery materials.

In 2011, S. A. Hong et al[32] have reported nanosize lithium iron phosphate ($LiFePO_4$) particles using a continuous supercritical hydrothermal synthesis method at 25MPa and 400 ◦C under various flow rates. The authors have used modified continuous process to control the properties of $LiFePO_4$ in supercritical water including purity, crystallinity, atomic composition, particle size, surface area, and thermal stability, which are compared with the $LiFePO_4$ prepared via solid state method.

SEM images of the $LiFePO_4$ particles prepared using the Supercritical hydrothermal synthesis method are shown in **Fig.12(A)-(C)**. The particle size with 200-800 nm is obtained with the lower precursor solution flow rate (1.7 $gmin^{-1}$) as shown in **Fig.12A**. When the higher precursor solution flow rate (3 $gmin^{-1}$), the synthesized particles are uniform and smaller size particles with soft aggregation. When the water flow rate increased from 9 $gmin^{-1}$ to 18 $gmin^{-1}$, the particles are smaller with rod-shape morphology were observed(**Fig.12C**).

The cyclic performance of $LiFePO_4$ particles synthesized at three different precursor solution flow rate(**Fig.12**(**A**)-(**C**)) are shown in **Fig.12D**, the results are compared with $LiFePO_4$ particles prepared by solid state reaction method. $LiFePO_4$ particles (**Fig.12A-C**) show low initial capacity compared to the solid-state synthesized $LiFePO_4$ (sample S, in **Fig.12D**), which may be because the presence of the Fe^{3+} impurities in the as-synthesized $LiFePO_4$ particles.

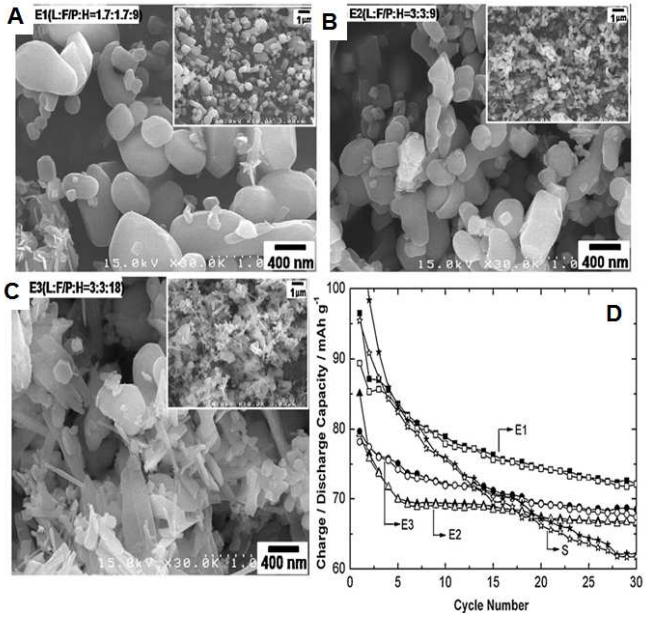

Fig.12 (A)-(C) SEM images of $LiFePO_4$ particles synthesized via supercritical hydrothermal synthesis method with different flow rate and (D) cyclic performance of $LiFePO_4$ particles shown in Fig.12(A)-(C) in comparison with $LiFePO_4$ prepared via solid state reaction method. (Reprinted with permission from Elsevier Ltd.)[32]

However, $LiFePO_4$ prepared with lower precursor solution flow rate (1.7 $gmin^{-1}$, E1 in **Fig. 12D**) showed larger capacities after 6 cycles and $LiFePO_4$ prepared with higher precursor solution flow rate (9 $gmin^{-1}$, E2 in **Fig. 12D** and 18 $gmin^{-1}$, E3 in **Fig. 12D**) showed larger capacities after 16-20 cycles over the $LiFePO_4$ prepared via solid state reaction method. The better cycle performance of the as-synthesized $LiFePO_4$ particles can be due to more homogeneous utilization of the active materials and shorter diffusion length of Li^+ ions associated with the smaller size particles. The authors observed high capacity after coating carbon to $LiFePO_4$ particles, the discharge capacities of 140-160 mA h g^{-1} was achieved for this materials. This results shows that, proper carbon coating to $LiFePO_4$ particle could leads to high discharge capacity. Further, in 2013, the same group[33] extended this work and investigated effect parameters such as, effect of reaction temperature, effect of precursor, effect of flow rate and effect residence time on $LiFePO_4$ nanoparticles. The authors able to improve the cyclic performance of carbon $LiFePO_4$ particles.

Recently, J. Yu et al[34] have synthesized spindle-like carbon coated $LiFePO_4$ ($LiFePO_4$/C) composites via a novel one-pot supercritical methanol method. $FeCl_2.4H_2O$, H_3PO_4, D-glucose and $LiOH.H_2O$ were used as starting materials. Methanol and Benzyl alcohol are used as solvents. **Fig. 13A** shows the XRD pattern of $LiFePO_4$/C particles synthesized using different concentration of Li source (L1, L2 and L3 patterns). The peak position and intensity of all the sample can be well indexed to standard $LiFePO_4$ peaks with olivine structure and belongs to space group *Pnma*. Some impurities phase around 26-30° was identified for L1-8wt% sample. Fig. 13B and 13D shows the TEM images of L2-8wt% and L3-8wt% samples, respectively. When the Li source is 20 mmol, the particles show microplate with spindle like morphologies with a length of several micrometers. However at high Li concentration (30 mmol), large scale well dispersed spindle like microstructures with few micrometer in length are observed as shown in Fig. 13C.

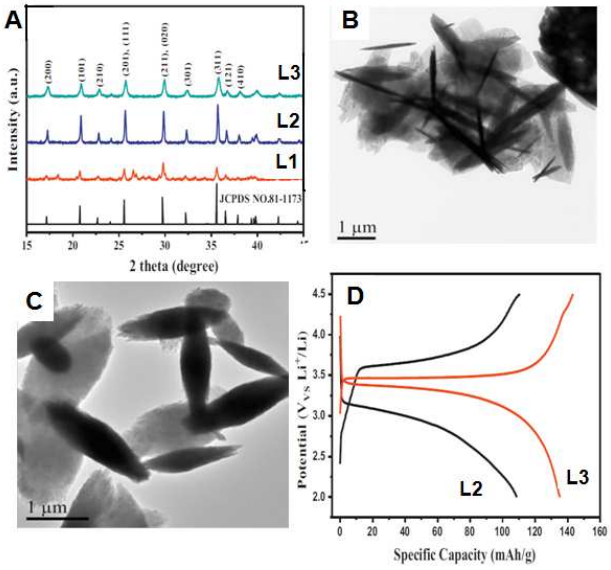

Fig.13 (A)XRD patterns of $LiFePO_4$ particles synthesized using different concentration of Li at one-pot supercritical methanol method, (B) and (C) TEM images of $LiFePO_4$ particles synthesized using 20 mmol and 30 mmol of Li source, (D) charge-discharge profile of $LiFePO_4$ particles shown in **Fig. 13B** and **13C**. (Reprinted with permission from Elsevier Ltd.)[34]

The charge discharge profile of LiFePO4 particles synthesized with Li source 20 mmol (L2 in **Fig. 13D**) and 30mmol(L3 in **Fig. 13D**) shown in **Fig. 13D**. The charge-discharge measurement was carried out between 2.0 to 4.5V. The discharge capacity of 108 and 135 mA h g^{-1} was observed at 0.2C for L2 and L3 samples shown in **Fig. 12D**. This results suggest that, $LiFePO_4$ particles with different morphologies with proper carbon coating could produce high capacity.

In 2013, M. Xie et al[35] have reported a template free method to prepare porous $LiFePO_4$ via supercritical carbon dioxide. The author propose follwing mechanism to synthesized porous $LiFePO_4$ particles by introducing $scCo_2$. First, $LiFePO_4$ was prepared by hydrothermal method and then followed by $scCo_2$ treatments in a supercritical fluid reactor. **Fig. 14A** shows the mechanism for synthesis of porous $LiFePO_4$ under supercritical carbon dioxide conditions. A1 sample is as-prepared $LiFePO_4$ by hydrothermal method, which was treated without $scCO_2$ (A2) and with $scCO_2$ at 100 bar 24h (A3), 100 bar for 48 h (A4), and 250 bar for 48 h (A5) at 100 ^oC. **Fig. 14B** shows the XRD patterns of sample A1-A5. The observed diffraction peaks are well matched with standard $LiFePO_4$ with orthorhombic structure (JCPDS 40-1499). All the characteristics peaks are clearly indexed to standard pattern. No impurity was found and the authors claim that introducing $scCo_2$ (Supercritical carbon dioxide) did not introduce any new phase or impurity phase in the synthesized cathode materials.SEM image shown in Fig. **14C** and **C1**, exhibited porous structures, when heating time reached 48 h under pressure of 250 bar. This sample exhibited BET surface area is about 28.7 m^2 g^{-1} which four time higher than that of A1 sample.

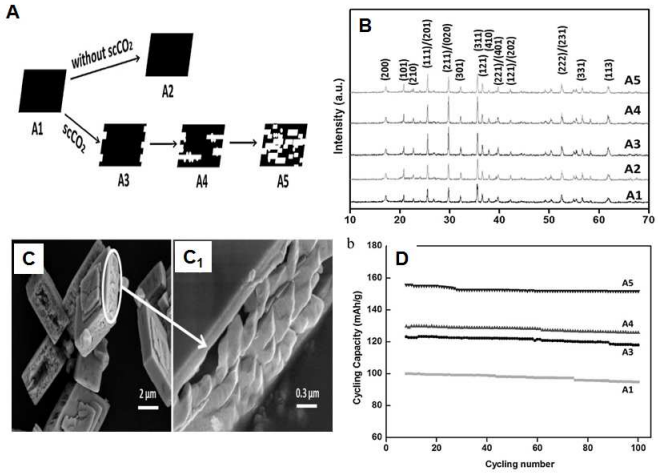

Fig.14 (A) Showing mechanism to synthesize porous $LiFePO_4$ particles by introducing $scCO_2$, (B) XRD patterns of A1-A5 samples, (C and C1) SEM images of porous $LiFePO_4$ particles, (D) cyclic performance of A1-A5 samples. (Reprinted with permission from Elsevier Ltd.)[35]

The cyclic performance shown in **Fig. 14D**, clearly indicating that, the porous $LiFePO_4$ particle had better cyclic performance than other samples. A5 sample exhibited 162 mA h g^{-1} for first cycle with little capacity fade, it shows high capacity due to its dominant porous structure compared to other samples. However, all the sample showed better cyclic performance than the non porous $LiFePO_4$ prepared via hydrothermal method. This investigation shows the importance of porous structure for energy storage applications.

In 2013, X. Rui et al[36] have proposed olivine-type nanosheets for lithium ion battery cathodes. They used a liquid-phase exfoliation approach combine with a solvothermal lithiation process in high pressure high-temperature (HPHT) supercritical fluids for the fabrication of $LiMPO_4$ nanosheets with thickness

of 3.7-4.6 nm with exposed (010) surface facets. The synthetic strategy for $LiMPO_4$/C nanosheets is depicted in **Fig. 15A**. The authors used bulk $NH_4FePO_4.H_2O$ which was synthesized by solid state reaction methods[36], then it was swelled by intercalating formamide molecules followed by ultrasonication for exfoliation, The exfoliated nanosheet were immersed into an ethanol solution containing PVP. Finally, the HPHT (10 MPa, 400 ^oC) solvothermal lithiation converted PVP-capped $NH_4FePO_4.H_2O$ nanosheets into $LiFEPO_4$/C nanosheets.

Fig. 15B-D shows the TEM images of $LiMnPO_4$/C, $LiCoPO_4$/C and $LiNiPO_4$/C nanosheets, respectively. The results reveal that the nanosheets morphology retain after the calcinations process. The SAED patterns (Insets in **Fig. 15B-D**) taken from individual nanosheets exhibit single crystalline properties, The interlayer spacing in the HRTEM images in Fig. 15E-G, are measured to be 0.21, 0.23 and 0.21 nm, respectively.

Fig. 16 shows the charge discharge and cyclic performance of $LiFePO_4$/C (A and D), $LiMnPO_4$/C(B and E) and $LiCoPO_4$/C (C and F) nanosheets, respectively.

The initial discharge capacities of 164, 157, and 153mA h g^{-1} at current density of 0.2C with columbic efficiency of 98%, 93%, and 88% for $LiFePO_4$/C, $LiMnPO_4$/C, and $LiCoPO_4$/C nanosheets are observed, respectively. In addition, nanosheets exhibited good cycling stabilities (**Fig. 16D-F**). The discharge capacities of 163, 147, and 136 mA h g^{-1} retained even at 50th cycle under a rate of 0.2 C for $LiFePO_4$/C, $LiMnPO_4$/C, and $LiCoPO_4$/C nanosheets, respectively. This results shows the importance of nanosheets like morphologies for rapid lithium ion mobility and electron mobility leads to high capacity due to their shortening *b* plane in nanosheets.

In 2012, synthesis of plate like $LiCoPO_4$ nanoparticles were reported by our group.[38a] For the synthesis of plate like $LiCoPO_4$ particles, $CoCl_2{\cdot}6H_2O$, H_3PO_4 and lithium acetyl acetonate were used as starting materials in 1:1:1 molar ratio. Oleylamine was used both as surfactant and reducing agent and ethanol was used as solvent. The synthesis was carried out at 400 ^oC for 4min using batch type reactors. Oleylamine played a important role in controlling the particles shape from sphere to plate and size from 50 nm to 200 nm. **Fig. 17A** shows the schematic illustrations of formation of plate like $LiCoPO_4$ particles under supercritical conditions, under supercritical conditions metal ions and oleylamine interaction took place and oleylamine molecules capped on to selective surface of metal ions to determine the particle shape as shown in **Fig. 17 A**. **Fig. 17B** shows the TEM image of plate like $LiCoPO_4$ particles, the particles showed 50-200 nm in width, 100-200 nm in length and side length from 5-15 nm. The side length is along *b* axis, which enhances the mobility of lithium ions during electrochemical reaction. **Fig. 17C** shows the charge discharge profile of plate like $LiCoPO_4$ particles measured at 0.05C, the first cycle discharge capacity of 135 mA h g^{-1} and 10th cycle discharge capacity of 89 mA h g^{-1} was observed with moderate cyclic performance. We believe that, the observed capacity is due to the plate like morphology, which has the particular advantages for lithium ion mobility. After motivated by this results, in 2014 we have investigated the effect of different kind of surfactants on shape of $LiCoPO_4$ particles.[38b] For the synthesis, cobalt acetate tetrahydrate ($Co(Ac)_2.4H_2O$) and lithium acetylacetonate were dissolved in 15 ml ethanol and the solution was heated at 60°C with continuous stirring. The synthesis was carried out at 400 ^oC for 6 min using batch type reactors. and nanoplates show higher discharge capacities than the nanoparticles, which is due to their short b axis length which reduce the lithium ion mobility path to result in higher discharge capacities. The moderate cyclic performance is observed for nanorods and nanoplates as shown in **Fig. 18E**. From this results, we have demonstrated that, controlling morphology and size of $LiCoPO_4$ cathode materials are important to enhance the electrochemical performance of the cathode materials.

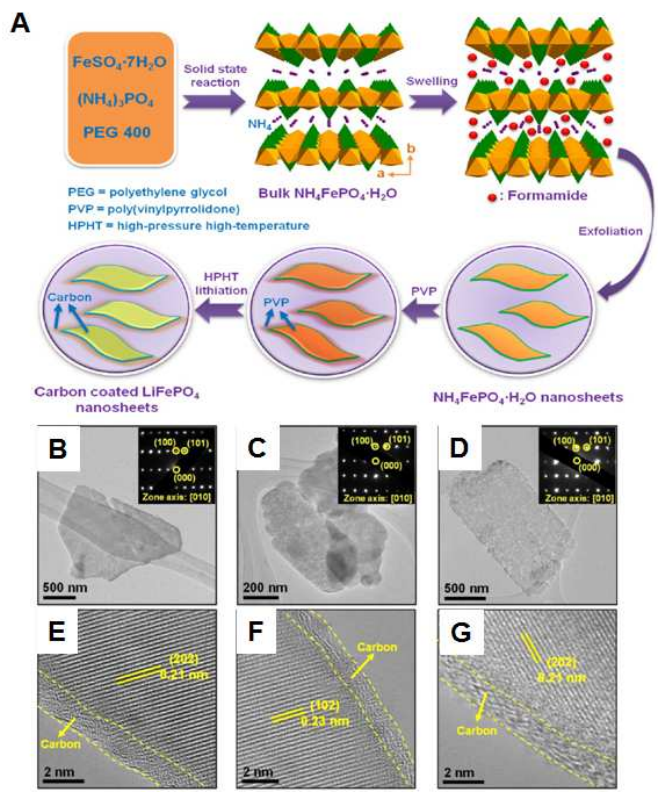

Fig.15 (A) Schematic illustration of the preparation of carbon-coated $LiFePO_4$ nanosheets through a liquid-phase exfoliation approach combined with a HPHT solvothermal lithiation process,(B-D) TEM images and (E-G) HRTEM images of $LiMnPO_4$/C (B and E), $LiCoPO_4$/C (C and F) and $LiNiPO_4$/C(D and G) particles. (Reprinted with permission from American Chemical Society.)[37]

Journal Name RSCPublishing

ARTICLE

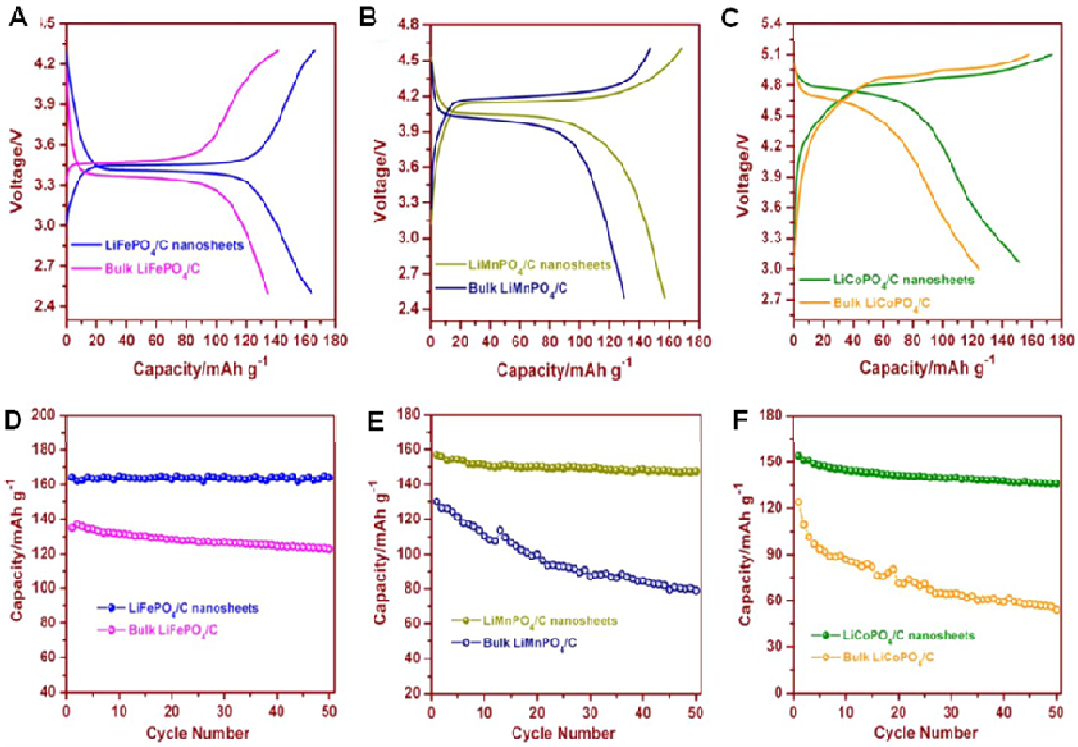

Fig. 16 Charge discharge profile and cyclic performances of $LiFePO_4$/C (A and D), $LiMnPO_4$/C (B and E) and $LiCoPO_4$/C (C and F) nanosheet cathode materials. (Reprinted with permission from American Chemical Society.)[37]

Hexamethylenetetraamine (HMT) or hexamethylenediamine (HMD) were used as in situ OH^- sources and structure-directing agent to control the growth rate as well as morphology of $LiCoPO_4$ particles.

Fig. 18A shows the mechanism of formation of $LiCoPO_4$ with three different kinds of morphologies such as nanoparticle, nanorod and nanoplate. HMT played an important role in controlling the size of the synthesized $LiCoPO_4$ particles. Under supercritical conditions, generated NH_3 from HMT provided the basic conditions for the crystallization of LiCoPO4 particles and the in situ release of ammonia and OH^- anions promote the formation of nanoparticles. HMD acted as shape-controlling agent to regulate the crystallographic orientation of the $LiCoPO_4$ nanocrystals under supercritical conditions and resulting in the formation of nanorods with 500 - 1000 nm in length, 50 nm in thickness and nanoplates with 500 nm in length, 200 nm in width and 50 nm in thickness as shown in Fig. 18B and 18C, respectively. **Fig. 18D** and **18E** shows the charge-discharge profile and cyclic performance of $LiCoPO_4$ nanoparticles, nanorods and nanoplates. The discharge capacities of 105, 130 and 121 mA h g^{-1} was observed. Interestingly, nanorods exhibited highest discharge capacities than the nanoparticles and nanoplates. However, both nanorods and nanoplates show improved discharge capacity with moderate cyclic performance than the $LiCoPO_4$ nanoparticles.

From the above discussion, we can observe that supercritical fluid process is one pot synthesis for lithium metal phosphates with well controlled size and morphology with excellent electrochemical properties. The carbon coating of lithium metal phosphates is very crucial in order to improve cyclic performance and rate performance. Many of the above discussed papers show the effect of carbon coating design on performance improvement of lithium metal phosphates. The different carbon sources have been effectively used for the performance improvement of lithium metal phosphates, specially for the $LiFePO_4$ cathode materials.

The electrochemical property of $LiMnPO_4$, $LiCoPO_4$ and $LiNiPO_4$ cathode materials must be improved for further utilization of these materials in lithium ion battery applications. Especially for high voltage applications, $LiCoPO_4$ and $LiNiPO_4$

cathode materials should be continued and electrochemical performances should be measured using high voltage electrolyte, solid electrolyte and ionic liquid electrolyte.

5. Lithium metal fluorophosphates

Recently, lithium metal fluorophosphates have been considered as possible promising candidates as high-energy-cathode materials for lithium ion batteries.[39] Three dimensional Li ion transport and one dimensional electron transport is expected for fluorophosphates because of one-dimensional chains of metal octahedra interconnected by polyanion tetrahedra.[39b] High specific capacity about 290 mA h g^{-1} is expected, if it is possible to incorporate a second Li^+ ion in Li_2MPO_4F (M = Fe, Co, Mn) materials to get high capacity than the olivine structured phosphate materials.
Usually, Li_2MPO_4F (M = Fe, Co, Mn) materials are prepared by low temperature solution synthesis followed by heat

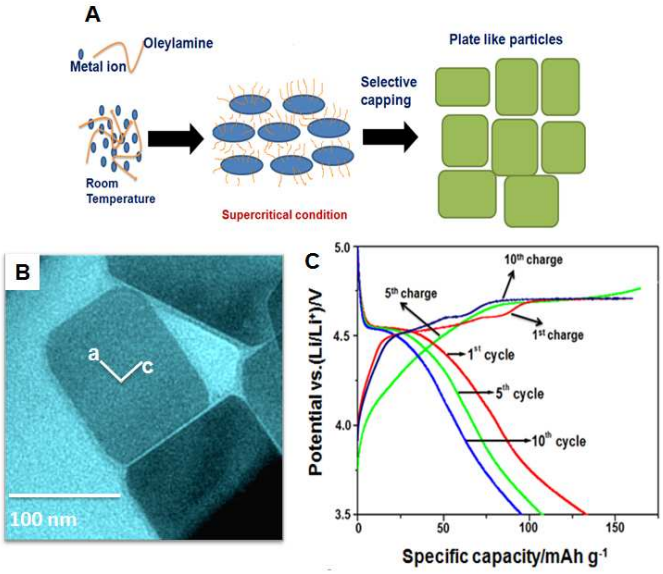

Fig.17 (A) Schematic illustration of formation mechanism of plate like $LiCoPO_4$ nanoparticles at supercritical solvothermal condition,(B) TEM images of plate like $LiCoPO_4$ particles and (C) Charge-discharge profile of conductive carbon coated $LiCoPO_4$ particles.(Reprinted with permission from Elsevier Ltd.)[38a]

treatment or solid state reaction methods. For the first time, in 2013 we proposed one pot supercritical fluid process to synthesize Li_2FePO_4F at 400 °C for about 10-30min using batch reactors.[40]
The synthesis of single phase Li_2FePO_4F cathode materials is not easy without the adaptation of special synthetic conditions and careful selection of the starting materials. For the synthesis, Iron chloride (II) tetrahydrate ($FeCl_2.4H_2O$), orthophosphoric acid (H_3PO_4) and lithium fluoride (LiF) were used in in 1:1:4 molar ratios. Ascorbic acid was used as reducing agent, water and ethylene glycol were used as solvents. **Fig. 19A** shows the XRD pattern of as-synthesized Li_2FePO_4F nanoparticles under supercritical fluid conditions at 400 °C using water and EG as solvents for 10 min and 30min of reaction time. The XRD pattern were compared to XRD patterns reported by Nazar et al.[39a] Selected diffraction peaks (inset figure in **Fig. 19A**) confirm the formation of Li_2FePO_4F and reveal that Li_2FePO_4F belongs to the $P\bar{1}$ space group with triclinic crystal system. The crystal structure of Li_2FePO_4F inserted in **Fig. 19A** shows the arrangement of the iron octahedra, phosphate tetrahedra and Li ions. **Fig. 19B** shows the TEM image of Li_2FePO_4F nanoparticles synthesized at 400 °C for 30min of reaction time. The particles showed 80-150 nm in diameter with octahedral shape and show well developed crystal habit. The charge-discharge performance of Li_2FePO_4F nanoparticles at 50 °C is shown in **Fig. 19C**, the discharge capacity of 148 mA h g^{-1} is noticed with good cyclability than the discharge capacity of Li_2FePO_4F nanoparticles measured at room temperature (**Fig. 19D**).

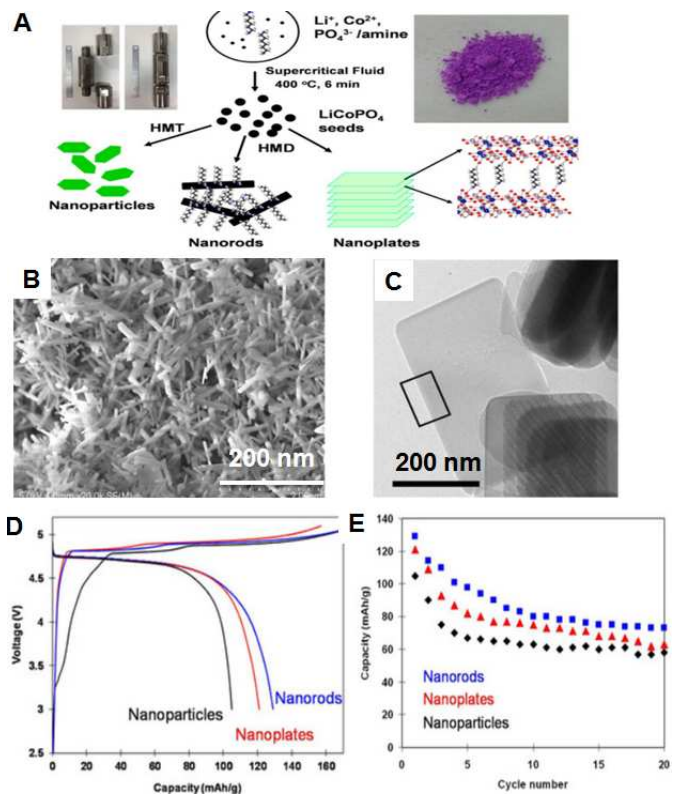

Fig. 18 (A) Schematic illustration of formation mechanism of $LiCoPO_4$ nanoparticles, nanorods and nanoplates at supercritical condition, batch reactors and image of $LiCoPO_4$ powder (B) TEM images of rod like $LiCoPO_4$ particles and (D) and (E) Charge-discharge profile and cyclic performance of $LiCoPO_4$ nanoparticles, nanorods and nanoplates.(Reprinted with permission from Elsevier Ltd.)[38b]

The obtained capacity is almost near to one lithium ion capacity of Li_2FePO_4F cathode material. The increased

discharge capacity at elevated temperature might be due to the increase in the electronic conductivity and also due to the nanosize effect, where the length of the lithium ion diffusion is shortened in the Li_2FePO_4F nanoparticles.

Easy and cheap synthesis methods should be developed for the synthesis of flurophosphates because few reported methods demonstrate two to three step synthesis routes. The focus on utilization of second lithium ion would be very useful in order to effective use of these cathode materials for high capacity applications.

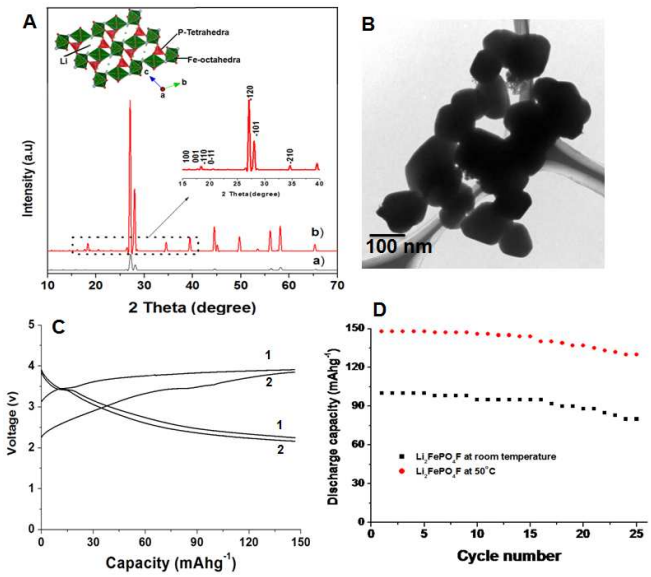

Fig.19 (A) XRD pattern and crystal structure of Li_2FePO_4F nanoparticles synthesized at supercritical fluid process (a-10min, b-30min),(B) TEM images of Li_2FePO_4F nanoparticles synthesized in 30min, and (C) Charge-discharge profile (at 50 ^oC) and cyclic performance of Li_2FePO_4F nanoparticles.(Reprinted with permission from Royal Society of Chemistry.)[40]

6. Lithium metal silicates

After successful development of olivine structured cathode materials, lithium orthosilicate, Li_2MSiO_4 (M = Fe, Mn and Co), based cathodes have attracted as promising lithium ion battery materials due to their fabulous advantages such as high theoretical capacity (>330 mA h g^{-1} which is possible while extracting more than one Li^+ ion per formula unit), high thermal stability through strong Si–O bonding, safety, cost effectiveness, as well as being eco-friendly and easy to synthesize.[41]

In 2012, we have proposed supercritical fluid process for synthesis of Li_2MSiO_4 (M = Fe and Mn) nanosheets for the first time.[42] Earlier, only solid state reaction method and low temperatures methods have been adopted for the synthesis of Li_2MSiO_4 (M = Fe, Mn and Co), based cathodes.[41]

Li_2MSiO_4 (M = Fe and Mn) nanosheets were synthesized from $FeCl_2.4H_2O$, tetraethylorthosilicate(TEOS) and LiOH. H_2O in 1:1:4 molar ratio. Ethanol and water were used as solvents for the synthesis. The synthesis was carried out at 350-420 ^oC for about 4-10 min of reaction time. TEM images of the as-synthesized Li_2FeSiO_4 and Li_2MnSiO_4 nanosheets are shown in **Fig. 20A-20D**. The low magnification images (**Fig. 20A** and 20C) shows the observed sheet like structures are the predominant morphology of the particles and few sheets are rolled up. The closer lobservation shows that the 2-D nanosheets binded together to form a bundle of agglomerated sheets (**Fig. 20B and 20D**). The nanosheets show few atomic thick sheets with lateral dimensions of 100-300 nm in length and 1-5nm in thickness, which is very beneficial for electron transport and for the lithium ion mobility across b axis of Li_2FeSiO_4 and Li_2MnSiO_4 cathodes.

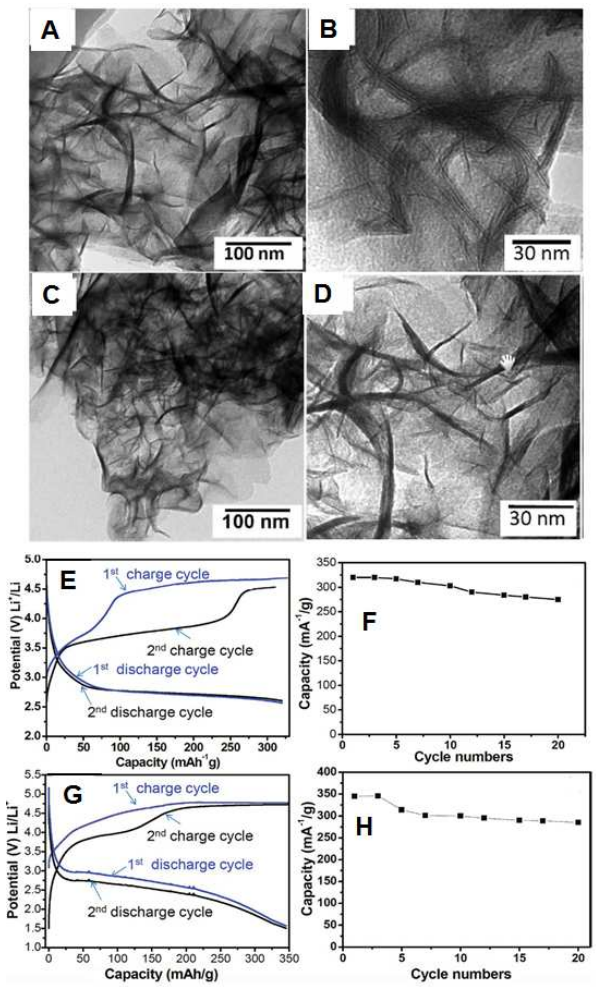

Fig. 20 (A-D) TEM images Li_2FeSiO_4 nanosheets (A and B), Li_2MnSiO_4 nanosheets (C and D) of synthesized at supercritical fluid conditions, and (E-H) Charge-discharge profile and cyclic performances of Li_2FeSiO_4 nanosheets (E and F), Li_2MnSiO_4 nanosheets (G and H) (Reprinted with permission from American Chemical Society.)[42]

The discharge capacities of 340 mA h g^{-1} and 350 mA h g^{-1} at 45 ±5 ^oC with good cyclability were recorded for the Li_2FeSiO_4 (**Fig. 20E** and **20F**) and Li_2MnSiO_4 (**Fig. 20G** and **20H**) nanosheets, respectively. This observed specific capacity is

more than the theoretical capacity involving 2 lithium ion in Li_2MSiO_4 (333 mA h g^{-1}), this results indicated the ability of 2 lithium ion extract/insert in sheet like electrodes due to the oxidation state of $Fe^{3+/4+}/Mn^{3+/4+}$ couple at the high temperatures. The achievement of full theoretical capacity is due to the fast lithium ion transport in sheet like structure with 1-5nm of b-axis thickness. The cyclic performance show small capacity loss after few cycles, and more than 1.6 lithium ion capacity is still observed at 20th cycle due to the nanosheet morphology of Li_2FeSiO_4 and Li_2MnSiO_4 cathodes.

In 2012, we have investigated controlled synthesis of nanocrystalline Li_2MnSiO_4 particles via supercritical solvothermal method using batch type reactors.[43] Li_2MnSiO_4 nanoparticles were prepared from manganese chloride (II) tetrahydrate, tetra ethyl orthosilicate (TEOS) and Lithium hydroxide in 1:1:4 molar ratios. Ethanol-water were used as solvents and ascorbic acid was used as reducing agent. The synthesis was carried out at 300 ^oC for 5min. **Fig. 21** shows the TEM image of as-synthesized Li_2MnSiO_4 particles, the particles showed spherical morphology with 5-20 nm in diameter. The particles are monodispersed and non-aggregated due to the effect of dielectric constant of ethanol-water mixed solvents under supercritical conditions. The Li_2MnSiO_4 nanoparticles were PEDOT coated for electrochemical analysis. The charge-discharge profile of Li_2MnSiO_4 nanoparticles measured at 40 ^oC, showed first discharge capacity of 313 mA h g^{-1} and 282 mA h g^{-1} for the second discharge at 0.05C (**Fig. 21**). The observed capacity is higher than many reported value and higher discharge capacity is achieved for Li_2MnSiO_4 nanoparticles due to its monodispersed particle size followed by PEDOT coating.

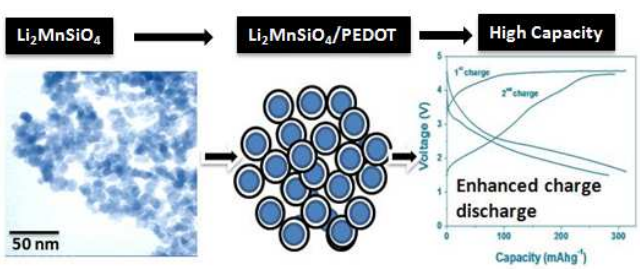

Fig. 21 TEM images Li_2MnSiO_4 nanoparticles, followed by PEDOT coating and charge-discharge profile of Li_2MnSiO_4 nanoparticles at 40 ^oC (Reprinted with permission from Royal Society of Chemistry.)[43]

After motivated by size and morphological effect on electrochemical performances of Li_2MnSiO_4 nanoparticles, In 2013, we have synthesized various sizes and morphologies of Li_2MnSiO_4 nanoparticles.[44] For the synthesis of Li_2MnSiO_4 cathode material, manganese chloride (II) tetrahydrate, tetra ethyl orthosilicate (TEOS) and lithium hydroxide in 1:1:4 molar ratios. Water, diethylene glycol, ethylene glycol with different volume ratios were used as solvents. Oleic acid and oleylamine were used as surfactant and reducing agents. The synthesis was carried out at 400 ^oC for 4 -30min.

Fig. 22 shows the TEM images of various size and morphologies of Li_2MnSiO_4 nanoparticles under supercritical fluid process. Ultrafine particles of 4-5 nm in diameter with uniform shape and size distribution were synthesized using water and diethylene glycol as the solvent and oleic acid as the surfactant. Oleic acid and diethylene glycol play a key role in restricting the particle size and shape under supercritical fluid conditions. Li_2MnSiO_4 hierarchical nanostructures with sunflower like morphology were obtained using high amount of oleic acid at 400 ^oC for 4min. Each flower measuring 200-400 nm in size and they are self assembled as hierarchical nanostructures. A possible reason for formation of hierarchical nanostructures is the self-assembly of monodispersed nanoparticles. The increased amount of oleic acid and low dielectric constant of organic solvents may facilitate a strong interaction between the metal nanoparticles and connects them to promote the formation of hierarchical nanostructures. The Li_2MnSiO_4 particles with 15-100 nm size with sphere like morphologies were also synthesized using difference combination of water and organic solvent under supercritical fluid process as shown in **Fig. 22**. The cyclic performances of monodisperse nanoparticles (4-5 nm), hierarchical nanostructures and 30-50 nm size Li_2MnSiO_4 particles are shown in **Fig. 23**. The monodispersed nanoparticles showed high initial discharge capacity of 292 mA h g^{-1} and discharge

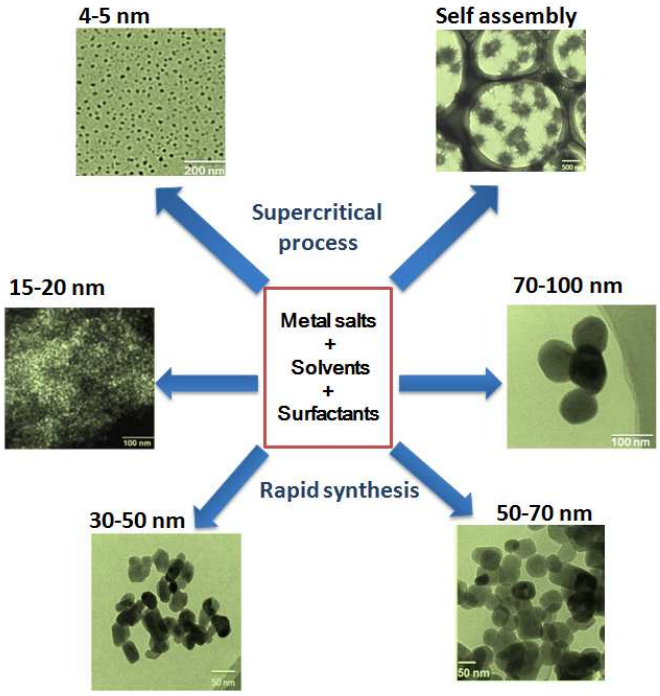

Fig. 22 TEM images of different size and morphlogies of Li_2MnSiO_4 nanoparticles, (Reprinted with permission from Royal Society of Chemistry.)[44]

capacity decreased after few cycles due to the detachment of nanoparticles from carbon matrix. However the discharge capacity of 184 mA h g^{-1} with good cyclabiltiy is observed. Hierarchical nanostructure exhibited the discharge capacity of 283 mA h g^{-1} for the first cycle and discharge capacity decreased after few cycle, and a stable cyclability and discharge capacity of 220 mA h g^{-1} was observed at 50th cycle.

Li_2MnSiO_4 particles with 30-50 nm size showed initial discharge capacity of 222 mA h g^{-1} and discharge capacity decreased after few cycles, and stable cylic performance with one lithium ion capacity was observed. However, highest capacity and better cyclability is observed for both monodisperse and hierarchical nanostructures. These results again demonstrated the effect of size and morphologies on electrochemical performances.

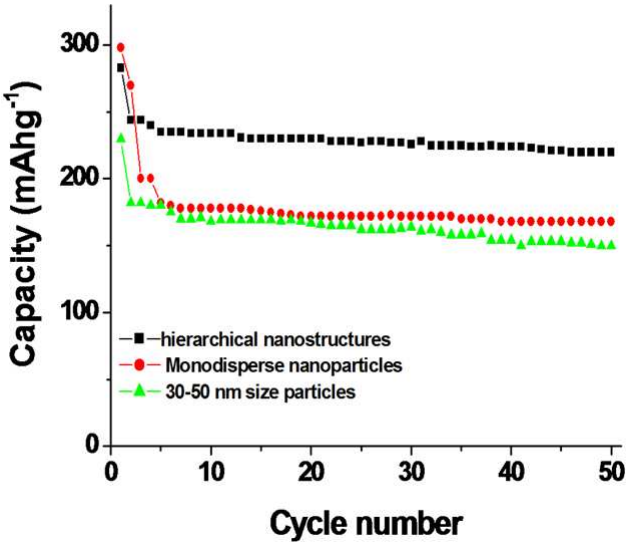

Fig. 23 TEM images of different size and morphologies of Li_2MnSiO_4 nanoparticles, (Reprinted with permission from Royal Society of Chemistry.)[44]

In 2013, we have proposed supercritical hydrothermal synthesis for Li_2FeSiO_4 rod like particles.[45] Li_2FeSiO_4 particles were synthesized from iron chloride (II) tetrahydrate, tetra ethyl orthosilicate (TEOS) and lithium hydroxide monohydrate in 1:1:4 molar ratios. Water was used as solvent and ascorbic acid was used as reducing agent. 5 mg of sucrose was used as in-situ carbon source. The synthesis was carried out at 380 °C for 30 min of reaction time using batch type reactors.

Fig. 24A shows the as-synthesized Li_2FeSiO_4 particles at 380 °C for 30min, large number of particles having rod like morphology with diameter ranging from 20 to 60 nm and approximately 50-500 nm in length can be observed. The rod like Li_2FeSiO_4 particles are covered with amorphous carbon which is formed due to the ascorbic acid and sucrose decomposition products. **Fig. 24B** shows the single rod like Li_2FeSiO_4 particles synthesized at 380 °C is shown and the dot pattern obtained by electron diffraction (ED) clearly indicates that, the rod like Li_2FeSiO_4 particles are single crystalline in nature as shown in **Fig. 24B** (inset image). The HRTEM image shown in Fig.24C, clearly showing the well resolved lattice fringes suggesting the good crystallinity of Li_2FeSiO_4 particles.

The initial discharge capacity of 102 mA h g^{-1} at 0.05C is obtained for as-synthesized rod like Li_2FeSiO_4 particles with poor cyclability as shown in **Fig. 25A** and **25D**. The first discharge capacity of 118 mA h g^{-1} and 177 mA hg^{-1} 0.05 C was obtained for 20 wt% and 30 wt% conductive carbon coated rod like Li_2FeSiO_4 particles as shown in **Fig. 25B** and **25C**,

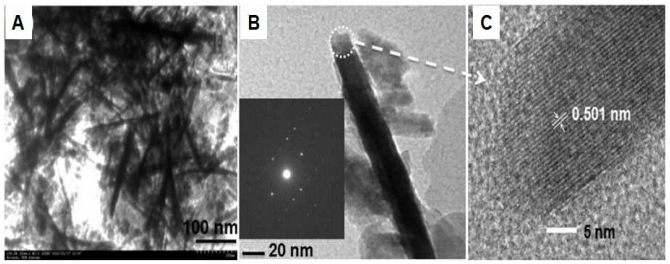

Fig. 24 (A)TEM images of rod like Li_2FeSiO_4 particles,(B) single rod like Li_2FeSiO_4 particle with ED pattern (inset) and (C) HRTEM image. (Reprinted with permission from Elsevier Ltd.)[45]

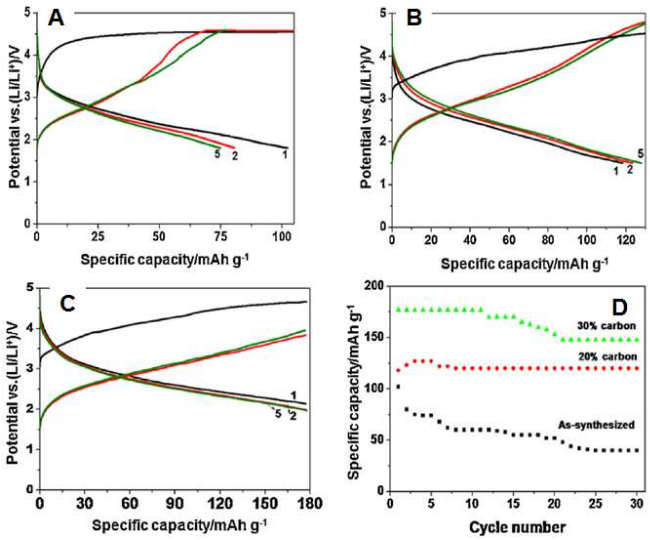

Fig. 25 (A)Charge-discharge profile of as-synthesized rod like Li_2FeSiO_4 particles,(B) 20 wt% carbon coated Li_2FeSiO_4 particle, (C) 30 wt% carbon coated Li_2FeSiO_4 particle and (D) cyclic performance of Li_2FeSiO_4 particle.(Reprinted with permission from Elsevier Ltd.)[45]

respectively. However, the discharge capacity of more than one Li^+ was observed even after several cycles for rod like Li_2FeSiO_4 particles (**Fig. 25D**) and this discharge capacity is nearly that of previously reported discharge capacity for Li_2FeSiO_4 cathode material.

In 2013, we extended supercritical fluid process to synthesize nanocrystalline Li_2CoSiO_4 particles.[46] Li_2CoSiO_4 nanoparticles were synthesized from cobalt(II) chloride hexahydrate, tetra

ethyl orthosilicate (TEOS) and lithium hydroxide (Wako, Japan) in a 1 : 1 : 4 molar ratios.Water-ethanol were used as mixed solvents and oleylamine was used as a reducing agent. The synthesis was carried out at 350 ^{o}C for 1h of reaction time. **Fig. 26A** shows the XRD patterns of as-synthesized (350 °C for 1 h) and heated (500 °C for 2 h) Li_2CoSiO_4 particles. The heating was carried out to remove surface absorbed organic derived residues from the Li_2CoSiO_4 particles and also to produce well crystallized particles for the structural investigation by ADF/ABF analysis. The as-synthesized and heated Li_2CoSiO_4 samples exhibited well defined diffraction peaks and XRD data matches well with the reported data and the JCPDS file (00-024-0608). Li_2CoSiO_4 belongs to the orthorhombic crystal system with a space-group of $Pbn2_1$. TEM image shown in **Fig. 26B** indicates the average particle sizes of Li_2CoSiO_4 particles between 50–250 nm with irregular shape, and the particles are well distributed without any agglomeration. Further, we also analyzed the structure of this materials via ADF/ABF and showed tetrahedral arrangements of SiO_4, LiO_4 and CoO_4.

The heated (500 °C for 2 h) Li_2CoSiO_4 particles shows the discharge capacity of nearly 107 mA h g^{-1} with gentle slope like profile for the first and second cycles as shown in **Fig. 26B**. The observed discharge capacity is much smaller than the theoretical capacity of 325 mA h g^{-1} (2 lithium extraction). In addition, the cyclic performance was observed to be very poor that after two cycles the discharge profile drops below 3V probably due to the structural collapse of this material on electrochemical analysis.

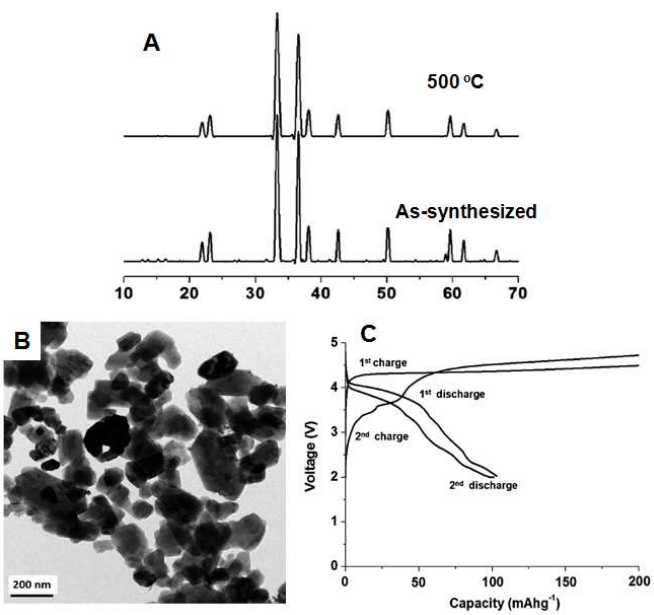

Fig. 26 (A)XRD pattern of as-synthesized and heated Li_2CoSiO_4 particles,(B) TEM image of Li_2CoSiO_4 particles (C) charge-discharge profile of Li_2CoSiO_4 particles.(Reprinted with permission Royal Society of Chemistry.)[46]

From the above discussion, it is clear that supercritical fluid process is beneficial for the synthesis of size, morphology and structure controlled synthesis of lithium metal silicates with observation of nearly full theoretical capacity. Further research has to be carried out because lithium metal silicates are very promising cathode materials, and the recent observation of two lithium capacity is motivate us to investigate more on these materials. The surface chemistry modifications and coating technology for this materials should be developed for future high capacity application in lithium ion battery.

7. Summary and outlook

In this review article, we have summarized the supercritical fluid methods used for the synthesis of lithium ion battery materials. In the beginning, we introduced briefly on different kind of supercritical fluid methods and supercritical fluid methods have been compared with other synthetic methods in terms of time and energy saving. Supercritical fluid methods using flow type reactors, batch type reactors and continuous supercritical synthesis process provides novel opportunity to synthesize lithium transition metal oxides in different size, morphology and with single phase, where the electrochemical performance greatly depend on the particle size and phase purity. Many researchers have successfully demonstrated the synthesis of $LiCoO_2$, $LiMn_2O_4$ and $LiNi_{1/3}Co_{1/3}Co_{1/3}O_2$ with particle size few nanometer to few micrometer. Good electrochemical performance for $LiCoO_2$, $LiMn_2O_4$ and $LiNi_{1/3}Co_{1/3}Co_{1/3}O_2$ were observed and compared to be higher than these materials synthesized via various synthetic routes. Further, lithium metal phosphates such as $LiFePO_4$, $LiMnPO_4$ and $LiCoPO_4$ cathode materials have been successfully synthesized by various research groups including our group. The particle size from 10-500 nm with different kind of morphologies such as sphere, rod, plate, colloidal particle, porous structure, spindle like and sheet like morphologies have been successfully developed. It was observed that, the electrochemical performances was mainly depended on size and morphology of these electrode materials. The colloidal $LiFePO_4$ particles, spindle like particle, porous particles and sheet like particles showed improved discharge capacities. The discharge capacity of 140-163 mA h g^{-1} with moderate to excellent cyclic performances has been observed. The discharge capacity of 60-160 mA h g^{-1} has been observed for 20-100 nm size particles and for sheet like particles. The plate like, sheet like and rod like $LiCoPO_4$ cathode materials with 5-15 nm thickness along b-axis showed improved discharge capacities of 90- 150 mA h g^{-1}, which were synthesized via supercritical fluid methods. For the first time, Li_2FePO_4F cathode material with 50-180 nm has been synthesized. Li_2FePO_4F showed discharge capacities of nearly one lithium ion has been observed at elevated temperature.

Lithium metal silicates such as Li_2FeSiO_4, Li_2MnSiO_4 and Li_2MnSiO_4 cathode materials have been investigated by our group for the first time via supercritical fluid process using batch type reactors. The Li_2FeSiO_4, Li_2MnSiO_4 with sheet like morphology showed nearly two lithium ion capacity and

monodispersed nanoparticles with 15-20 nm size particles also exhibited high capacity of more than 300 mA h g^{-1} for the first cycle discharge capacities. Ultrafine nanoparticles and hierarchical nanostructures exhibited stable cyclic performance due to their unique morphologies. For the first time, Li_2CoSiO_4 particles have been synthesized via supercritical fluid process with particle size 50-200 nm in size, a moderate discharge capacity with poor cyclic performances have been observed for this material.

Supercritical fluid methods have proved to be very beneficial in controlling the size and shape of the lithium battery materials. We hope that, this review provide useful information about materials process via supercritical fluid methods for energy storage applications and promising that this process could be extended for the synthesis of variety of technologically potential materials.

Acknowledgements

This work was supported by the Funding Program for World-Leading Innovative R&D on Science and Technology (FIRST), 'Innovative Basic Research Toward Creation of High-Performance Battery", from the Cabinet Office of Japan, and by the Grants-in-Aid for the Young Scientist (B) (23760656) and Exploratory Research (25630437) from the Japan Society for the Promotion of Science (JSPS).

Notes and references

[a] Institute of Multidisciplinary Research for Advanced Materials, Tohoku university, Katahira 2-1-1, Aoba-ku, Sendai 980-8577, Japan.
Tel: +81-8022-217-5186. Email: devaraju113@gmail.com; i.honma@tagen.tohoku.ac.jp

† Footnotes should appear here. These might include comments relevant to but not central to the matter under discussion, limited experimental and spectral data, and crystallographic data.

Electronic Supplementary Information (ESI) available: [details of any supplementary information available should be included here]. See DOI: 10.1039/b000000x/

1 J. Chen, *Recent Patents on Nanotechnology*, 2013, 7, 2.

2 S. Balaji, D. Mutharasu, N. Sankara Subramanian and K. Ramanathan, *Ionics*, 2009, **15**, 765–777.

3 (a) M.K.Devaraju and I. Honma, *Adv. Energy Mater*., 2012, **2**, 284. (b) M.K.Devaraju, M. Satish and I. Honma, (*Book Chapter*), Editors: J. Kauffman and K. M. Lee, Handbook of Sustainable Engineering, 2013, pp 1149-1173.

4 J. M. Tarascon and M. Armand, *Nature*, 2001, **414**, 359.

5 J. M. Tarascon, *Philos. Trans. R. Soc. London, Ser. A*, 2010, **368**, 3227.

6 (a) A. Burukhin, O. Brylev, P. Hany and B. R.Churagulov, *Solid. State.Ionics*. 2002,**151**, 259. (b) B. Huang, Y-I. Jang, Y-M. Chiang, D. R. Sadowa, *J. Applied. Electrochemistry*, 1998, **28**,1365.(c) L. Zhou, X. Zhou, X. Huang, Z. Liu, D. Zhao, X. Yao and C. Yu, *J. Mater. Chem. A*, 2013, **1**, 837.(d) G. H. Waller, S. Y. Lai, B.H. Rainwater, M. Liu, *J. Power Sources,* 2014, **251**, 411.(e) A. K. Padhi, K. S. Nanjundaswamy, and J .B. Goodenough, *J. Electrochem.Soc.*, 1997, **4**, 1188.(f) K. Zaghib, A. Mauger, F. Gendron, and C. M. Julien, *Chem. Mater.,* 2008, **20**, 462.(g) S.A. Hong, S.J. Kim, K.Y. Chung, M.S. Chun, B.G. Lee, J. Kim, *The J. of supercritical fluids*, 2013, **73**, 70.

7 (a) R. Dominko, M. Bele, M. Gaberscek, A. Meden, M. Remskar and J. Jamnik, *Electrochem. Commun*. 2006, **8**, 217. (b) A. Kokalj, R. Dominko, G. Mali, A. Meden, M. Gaberscek and *J.* Jamnik, *Chem. Mater*. 2007, **198**, 3633. (c) R. Dominko, *J. Power Sources.* 2008, **184**, 462. (d) R. Dominko, I. Arcon, A. Kodre, D. Hanzel and M. Gaberscek, *J. Power Sources.* 2009, **189**, 51. (e) Z. L. Gong, Y. X. Li, Y. Yang, *J. Power. Sources.* 2007, **174**, 524. (f) C. Lyness, B. Delobel, A. R. Armstrong and P. G. Bruce, *Chem.Commun*. 2007, 4890.

8 (a) B.L. Ellis, W.R.M.Makahnouk, Y. Makimura, K. Toghill, L.F. Nazar, *Nature Mater*., 2007, **6**, 749. (b) B.L. Ellis, W.R.M. Makahnouk, W.N. Rowan-Weetaluktuk, D.H. Ryan, L.F. Nazar, *Chem. Mater*. 2010, **22** 1059.(c) T.N. Ramesh, K.T. Lee, B.L. Ellis, L.F. Nazar, *Electrochem. Solid State Lett*., 2010, **13** , A43. (d) M.E.A. Dompablo, U. Amador, J.-M. Tarascon, *J. Power Sources*, 2007, **174**, 1251. (e) M. Ramzan, S. Lebegue, P. Larsson, R. Ahujia, *J. Appl. Phys*. 2009, **106** , 043510. (f) B. L. Ellis, T. N. Ramesh, W. N. Rowan-Weetaluktuk, D. H. Ryan and L. F. Nazar, *J. Mater. Chem*., **22**, 2012, 4759

9 (a) K. Amine, H. Yasuda and M. Yamachi, *Electrochem and Solid-State Lett*., 2000, **4**, 178. (b) P. Periasamy, B. RameshBabu, R. Thirunakaran, N. Kalaiselvi, T. Prem Kumar, N.G. Renganathan, M.Raghavan and N. Muniyandi, *Bull. Mater. Sci*., 2000, **23**, 345. (c) J. Wolfenstine, J. Read and J.L. Allen, *J. Power Sources*. 2007, **163**, 1070. (d) Z. Chen, Y. Ren, Y. Qin, H. Wu, S. Ma, J. Ren, X. He, Y.K. Sun, and K. Amine, *J. Mater. Chem*., 2011, **21**, 5604. (e) M. Prabua, M.V. Reddya, S. Selvasekarapandian, G.V. Subba Rao and B.V.R. Chowdari, *Electrochimica Acta*., 2012, **85**, 572.

10 D. Choi and P. N. Kumta, *J. Power. Sources*, 2007, **163**, 1064.

11 C. R. Sides, F. Croce, V. Y. Young, C. R. Martin and B. Scrosati, *Electrochem. Solid-State Lett*., 2005, **8**, A484.

12 G. Arnold, J. Garche, R. Hemmer, S. Strobele, C. Vogler, and A. Wohlfahrt-Mehrens, *J. Power. Sources*, 2003, **119**, 247.

13 S. Franger, F. Le Cras, C. Bourbon and H. Rouault, *J. Power. Sources*, 2003, **119**, 252.

14 J. K. Kim, G. Cheruvally, J. W. Choi, J. U. Kim, J. H. Ahn, G. B. Cho, K. W. Kim, H. J. Ahn, *J. Power. Sources*, 2007, **166**, 211.

15 H. C. Shin, W. I. Cho, H. Jang, *J. Power. Sources*, 2006, **159**, 1383.

16 M. Konarova, I. Taniguchi, *J. Power. Sources*, 2009, **194**, 1029.

17 (a) G. Meligrana, C. Gerbaldi, A. Tuel, S. Bodoardo and N.Penazzi, *J. Power. Sources* 2006, **160**, 516. (b) Y. S. Jeon, E. M. Jin, B. Jin, Dae-kyoo Jun, Z. J. Han and H. B. Gu, *Transactions on Electrical and Electronic Materials,* 2007, **8**, 41.(c) B. Ellis, W. H. Kan, W. R. M. Makahnouk and L. F. Nazar, *J. Mater. Chem*. 2007, **17**,3248. (d) C. Zhang, X. Huang, Y. Yin, J. Dai and Z. Zhu, *Ceram. Int*. 2009, **35**, 2979. (e) K. Saravanan, M. V. Reddy, P. Balaya, H. Gong, B. V. R. Chowdari and J. J. Vittal, *J. Mater. Chem*. 2009, **19**, 605. (f) Y. Wang, Y. Yang, Y. Yang, H. Shao, *Solid State Commun.,* 2010,**150**, 81-85. (g) A. V. Murugan, T. Muraliganth, P. J. Perreira, A. Manthiram, *Inorg. Chem*., 2009, 48, 946. (h) D. Rangappa, Koji Sone, T. Kudo, I. Honma, *J. Power Sources,* 2010, **195**, 6167. (i) D. Rangappa, M. Ichihara, T. Kudo and I. Honma, *J. Power. Sources,*

2009, **194**, 1036. (j) C. Wua, J. Xiea, G. Cao, X. Zhao and S. Zhang, *CrystEngCommn*., 2014, 10.1039/C3CE42377H. (k) K. M.O. Jensen, C T. M. Bremholm and B.B.Iversen, *CHEMSUSCHEM*, DOI: 10.1002/cssc.201301042

18 (a) M. K. Devaraju, S. Yin and T. Sato, *J. Crystal Growth*. 2009, **311**, 580. (b) M. K. Devaraju, S. Yin and T. Sato, Cryst.*Growth & Des*., 2009, **9**, 2944. (c) M. K. Devaraju, S. Yin and T. Sato, *ACS Applied Materials & Interfaces,* 2009, **1**, 2694. (d) M. K. Devaraju, X. Liu, K. Yusuke, S. Yin and T.Sato, T. *Nanotechnology,* 2009, **20**, 405606.(e) F. Cansell and C. Aymonier, *J. of Supercritical Fluids*. 2009, **47**, 508. (f) M. K. Devaraju, S. Yin and T. Sato, *Cryst.Eng.Com*., 2011, **13**, 741.(g) M. K. Devaraju, S. Yin and T. Sato, *Inorg Chem*., 2011, **50**, 4698. (h) T. Adschiri, Y. W. Leem M. Goto and S. Takami, *Green. Chem*., 2011, **13**, 1380.

19 (a) T. Adschiri, Y. Hakuta and K. Arai, *Ind. Eng. Chem. Res.,* 2000, **39**, 4901. (b) C. Aymonier, A. Loppinet-Serani, H. Rever´on, Y. Garrabos, F. Cansell, *J. of Supercritical Fluids*,2006, **38**, 242–251. (c) B. Veriansya, J-D. Kim, B.K. Min, Y.H. Shin and Y-W. Lee, J. Kim, *The J. Supercritical Fluids*, 2010, **52**, 76.

20 K. Kanamura, A. Goto, R. Young Ho, T. Umegaki, K. Toyoshima, K. Okada, Y. Hakuta, T. Adschiri, and K. Arai, *Electrochem. Solid State Lett*.,, 2000, **3** (6) 256.

21 T. Adschiri , Y. Hakuta, K. Kanamura and K. Arai, *High Pressure Research*, 2001. **20**, 373.

22 Y.H. Shin, S. M. Koo, D. S. Kim and Y.H. Lee, *J.of Supercritical Fluids*, 2009, **50**, 250.

23 K. Kanamura, K. Dokko and T. Kaizawa, *J.of the Electrochem.Soc*., 2005, **152**, A391.

24 J. H. Lee and J. Y. Han, *Korean.J.Chem.Eng.,* 2006, **23**(5), 714.

25 J. W. Lee, J. H. Lee, T. T. Viet, J.Y. Lee, J.S. Kim, *Electrochemica Acta*, 2010, **55**, 3015.

26 (a)J.Lee and A.S Teja, *J.of Supercritical Fluids*, 2005, **35**, 83-90. (b)J.Lee and A.S Teja, *Mater.Lett.,* 2006, **60**, 2105.(c) C.Xu, J. Lee and A.S Teja, *J.of Supercritical Fluids,* 2008, **44**, 92.

27 A. Aimable, D. Aymes, F. Bernard and F. Le Cras, *Solid State Ionics*, 2009, **180**, 861.

28 D. Rangappa, M. Ichihara, T. Kudo and I. Honma, *J. Power Sources*, 2009, **194**, 1036.

29 D. Rangappa, K. Sone, T. Kudo and I. Honma, *J. Power Sources*, 2010, **195**, 6167.

30 D. Rangappa, K. Sone, T. Kudo and I. Honma, *Chem. Commun.,* 2010, **46**, 7548.

31 D. Rangappa, K. Sone, Y. Zhou, T. Kudo and I. Honma, *J. Mater. Chem*., 2011, **21**, 7548.

32 S. A. Hong, S. J. Kim, K. Y. Chung, B. W. Cho and J. W. Kang, *J. of Supercritical Fluids,*2011, **55**, 1027.

33 S. A. Hong, S. J. Kim, K. Y. Chung, Y. W. Lee, J. Kim and B. Y. Sang, *Chem. Eng. J.,* 2013, **229**, 313.

34 J. Yu, J. Hu and J. Li, Applied Surface Science, 2012, **263**, 277.

35 M. Xie, X. X. Zhang, Y. Z.Wang, S.X. Deng, H. Wang, J.B. Liu, H. Yan, J. Laakso and E. Levanen, *Electrochimica Acta*, 2013, **94**, 16.

36 A. Q Yuan, J. Wu, L. J. Bai, S. M, Ma, Z. Y. Huang, Z. F. Tong, *Chem. Eng. Data*., 2008, **53**,1066.

37 X. Rui, X. Zhao, Z. Liu, H. Tan, D. Sim, H. H. Hng, R. Yazami, T.M. Lim and Q. Yan, *ACS Nano*., 2013, **7**(6), 5646.

38 (a)M. K. Devaraju, D. Rangappa and I. Honma. *Electrochimica acta.,* 2012, **85**, 548. (b) Q. D. Truong, M. K. Devaraju, Y. Ganbe, T. Tomai and I. Honma, *Scientific Reports*., 2014, **4**, 3975

39 (a) B. L. Ellis, T. N. Ramesh, W. N. Rowan-Weetaluktuk, D. H. Ryan and L. F. Nazar, *J. Mater. Chem.*, 2012, **22**, 4759.(b)T. N. Ramesh, K. T. Lee, B. L. Ellis and L. F. Nazar, *Electrochem. Solid-State Lett.*, 2010, **13**, A43–A47

40 M. K. Devaraju and I. Honma, *RSC Adv*., 2013, **3**,19849.

41 (a) R. Dominko, *Proc. SPIE*, 2010, **7683**, 76830J. (b) V. Aravindan, K. Karthikeyan, S. Ravi, S. Amaresh, W. S. Kim and Y. S. Lee, *J. Mater. Chem.*, 2010 **20**, 7340. (c) C. Deng, S. Zhang, B. L. Fu, S. Y. Yang and L. Ma, *Mater. Chem. Phys.*, 2010, **120**, 14. (d) K. Karthikeyan, V. Aravindan, S. B. Lee, I. C. Jang, H. H. Lim, G. J. Park, M. Yoshio and Y. S. Lee, *J. Alloys Compd.*, 2010, **504**, 224.

42 D. Rangappa, M.K.Devaraju, T. Tomai, A. Unemoto and I. Honma, *Nano Lett.*, 2012, **12**, 1146.

43 M. K. Devaraju, D. Rangappa and I. Honma, *Chem. Commun.,*2012, **48**(21), 2698.

44 M. K. Devaraju, T. Tomai, A. Unemoto and I. Honma, *RSC Adv.,*2013, **3**, 608.

45 M. K. Devaraju, T. Tomai and I. Honma, *Electrochimica Acta*., 2013, **109**, 75.

46. M. K. Devaraju, Q. D. Truong and I. Honma, *RSC Adv.*, 2013, **3**(43), 20633.

TOC graphic

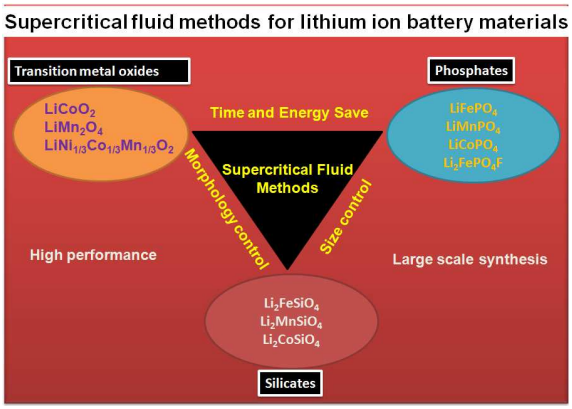

Synopsis:

Supercritical fluid methods have proved to be very beneficial in controlling the size and shape of the lithium battery materials. We hope that, this review provide useful information about materials process via supercritical fluid methods for energy storage applications and promising that this process could be extended for the synthesis of variety of technologically potential materials.